Nitrogen NMR Spectroscopy of Metal Nitrosyls and Related Compounds

Joan Mason,* Leslie F. Larkworthy, and Elaine A. Moore

Departments of Chemistry, Cambridge University, University of Surrey, The Open University, U.K.

Received November 15, 2001

Contents

I. Use of Nitrogen NMR Spectroscopy in Metal Nitrosyl Chemistry 913
A. Nitrogen NMR Spectroscopy: ^{14}N vs ^{15}N 913
B. Nitrogen Referencing 914
C. ^{15}N Relaxation 915
D. ^{15}N NOE Factors 916
E. ^{15}N Sensitivity Enhancement 917
F. Isotope Effects 918
G. Medium Effects 918
H. ^{14}N Line Widths: Quadrupolar Broadening 918
II. Preparation of ^{15}N-Enriched Metal Nitrosyls (L. F. Larkworthy) 919
A. Preparation of ^{15}N-Enriched Metal Nitrosyl 921
III. Patterns of Nitrogen Shifts in Metal Nitrosyls and Related Compounds 922
A. Nitrogen NMR Criteria of Structure 922
B. Coordination Shifts[2] 923
C. Ligand Field Effects in the Nitrogen and Metal Shielding 923
IV. Nitrogen Shielding Tensors in Metal Nitrosyls and Related Compounds[100] 924
A. Nitrogen Shielding Tensors in Linear Nitrosyls 925
B. Comparisons of ^{15}N and ^{13}C Shielding Tensors in Linear Nitrosyls (MNO) and Metal Carbonyls (MCO) 925
C. Nitrogen Shielding Tensors in Bent Nitrosyls 927
V. Theoretical Studies of Nitrogen Shielding Tensors in Metal Nitrosyls and Related Compounds (E. A. Moore) 929
VI. Patterns of Spin–Spin Couplings in Nitrosyls and Related Compounds[136] 931
VII. Dynamic Processes Observed in Nitrogen Resonance 932
VIII. References 933

I. The Use of Nitrogen NMR Spectroscopy in Metal Nitrosyl Chemistry

Nitrogen NMR spectroscopy[1,2] is peculiarly valuable in the chemistry of diamagnetic metal nitrosyls because of the sensitivity of nitrogen NMR parameters to the geometry at nitrogen, whether linear, bent or partially bent, fluxional, or bridging. NMR study, together with comparisons with related X−NO compounds, usefully supplements the information that can be gained from other forms of spectroscopy and structural studies.

Nitrogen shifts are readily interpreted by physical models which are familiar from the well-known $n_N-\pi^*$ excitations in electronic spectra, as described in sections III and V. The reason for this is that as linear MNO bends, π-bonding electron density moves to form lone pair (n) electron density on nitrogen, and the resulting $n_N-\pi^*$ circulations in the magnetic field, modulated by interaction with the d orbital system, are faithfully reflected in the nitrogen NMR spectrum, as they are in the optical spectrum. More detailed information is obtained from measurements of the ^{15}N tensors in the solid state, and these can provide evidence of spinning and wagging motions of the nitrosyl group in the crystal, as described in section IV. What is special about $n_N-\pi^*$ excitations in the −N=O group is their low energy: the (nonbonding) HOMO is high in energy and the LUMO is low because of the electronegativity of nitrogen and oxygen. Nitroso/nitrosyl compounds, therefore, tend to be colorful, and the nitrogen NMR shifts may be record-breaking.

Lone pair and/or π-electron density on nitrogen are involved also in associative properties which influence nuclear magnetic relaxation and, therefore, ^{14}N line widths and ^{15}N sensitivity. Dynamic processes also can be identified by NMR methods: thus, the swinging of a bent nitrosyl in the solid and bent−linear fluxionality in a bis-nitrosyl complex in solution were first identified through ^{15}N NMR, as described in section VII.

Much ^{15}N NMR work done on metal nitrosyls has involved nitrosylmetalloporphyrins, which are of considerable spectroscopic interest[3] in view of their use for model studies of bioregulatory processes involving NO[4] as also for O_2; much of the NMR work has involved cobalt, which is itself of biological interest, as in vitamin B_{12}.

A. Nitrogen NMR Spectroscopy: ^{14}N vs ^{15}N

Nitrogen NMR spectroscopy is well-documented with general reviews[5] and regular updating,[6] more specialized reviews,[7] including information on metal nitrosyl NMR,[8,9] two books entitled *^{15}N NMR Spectroscopy*,[10] and a wealth of older literature.[11]

Nitrogen NMR has not been used more widely in metal nitrosyl chemistry because of less-than-favorable NMR properties of the ^{14}N and ^{15}N nuclei, shown in Table 1. The highly abundant nucleus ^{14}N is quadrupolar, so lines given by molecules of the size of metal complexes may be very broad and broader for bent nitrosyls. However, the ^{14}N quadrupole moment is relatively small, and if the local symmetry is high, as in linear nitrosyls, and the molecule not

10.1021/cr000075l CCC: $39.75
Published on Web 03/26/2002

When Les Larkworthy and I met at UCL in the 1950s, I was making the first perfluoroalkyl nitroso compounds (CF_3NO, C_3F_7NO) using vacuum techniques I learned working with Emeléus in Cambridge, then with Anton Burg in Southern California. I dropped out for 8 years to raise a family but managed to return to chemistry at the University of East Anglia, moving to the (new) Open University in 1970. When Les and I met again in the 1980s, I was studying nitrosyl compounds by nitrogen NMR and he was making some very interesting metal nitrosyls. Chris Groombridge measured nitrogen shielding tensors for us, Mike Mingos thought up more examples of nitrosyl fluxions, and Elaine Moore took a useful interest in theoretical studies of nitrosyl compounds. Experiencing vicissitudes of the scientific career for women—I had to get a Cambridge ScD to become a Reader (= Associate Professor)—I now support the work of the Association for Women in Science and Engineering.

Leslie Larkworthy was born in 1930 in Plymouth, England, won a scholarship in 1948 to University College London, and worked on diazotization mechanisms with E. D. Hughes for his Ph.D. Joan Mason was at UCL at this time, and they used to chat while he used the colorimeter in the laboratory where she had built her vacuum line. He spend 3 years in the Royal Air Force as an education officer, returning to UCL in 1956 to work with Ron Nyholm on an iron–indigo complex; this led to later research on transition-metal chemistry and metal nitrosyls. In 1959 he took up a lectureship in chemistry at the Battersea College of Technology, London, which moved to Guildford to become the University of Surrey. He was awarded the DSc of the University of London in 1975, having worked with 40 or so graduate students and research associates from around the world, leading to almost 150 publications, by retirement in 1996.

too bulky, ^{14}N work can be done in reasonably high resolution with mobile samples, as described below. Most of the earlier nitrogen NMR work was done in ^{14}N resonance: the first demonstration of the chemical shift was in a solution of $^{14}NH_4{}^{14}NO_3$.[12]

^{15}N is a useful spin-1/2 nucleus, but the natural abundance is low, one-third of that of ^{13}C, as is the receptivity, 2.2% of that of ^{13}C. Nowadays, however, the use of Fourier transform methods, superconducting magnets, wide-bore spectrometers, and clever pulse sequences have greatly improved the accessibility of ^{15}N work. With enrichment to 99%, the receptivity of ^{15}N is 6 times that of ^{13}C in natural abundance (Table 1). We show in section II that high ^{15}N enrichment in complexes of interest is neither difficult nor expensive, since ^{15}N-labeled sodium nitrite and ammonium salts are cheap.

For biological tracer experiments, the most stable radioisotope of nitrogen, ^{13}N, is inconvenient to work with, since the half-life is only 10 min. This increases the importance of NMR work, with ^{15}N labeling, and cheap labor is available from bacteria or plants consuming ^{15}N -enriched ammonium salts.

Elaine Moore's doctorate at Oxford with Peter Atkins was on the theory of electron spin polarization in radical reactions, and her postdoctoral research with Richard Moss at Southampton University was in relativistic quantum chemistry. She joined the Chemistry Department of the Open University in 1975 and now produces distance learning texts, videos, and CD-ROMs in chemistry and astronomy. Her research has covered theoretical aspects of NMR spectroscopy, from relativistic effects to applied computational chemistry, including the application of computational methods to the solid state (in collaboration with Mike Mortimer and Frank Berry in the Solid State Chemistry Group at the Open University). She is co-author, with her colleague Lesley Smart, of an undergraduate text book on Solid State Chemistry, now published in five languages, and has two teenage children.

B. Nitrogen Referencing

Several reference standards have been used in nitrogen NMR spectroscopy.[13] Consensus favors the use of neat liquid nitromethane, as external reference, since it is accurately reproducible and can be obtained enriched with ^{15}N or ^{2}D. The ^{15}N signal is little affected by proton decoupling, and the ^{14}N signal is quite sharp. Internal referencing is unsatisfactory because of medium effects (section I.G), which are large when nitrogen carries a lone pair and quite large when nitrogen carries π electrons: Table 2 illustrates this for nitromethane.

The use of ammonia or ammonium salts for nitrogen referencing (so as to give mainly positive shifts) is unsatisfactory because of medium effects: there is a difference of nearly 7 ppm from the nitrate to the chloride in saturated solutions. NMe_4Cl and NEt_4Cl are less subject to medium effects but are little used. Nitrate ion is susceptible to hydrogen-bonding, particularly in acidic solution.

Ammonia is unsuitable as a reference substance because of hydrogen bonding but is a useful 'theoreti-

Table 1. NMR Properties of the Nitrogen Nuclei[a]

	^{14}N	^{15}N	*cf* ^{13}C
spin I	1	1/2	1/2
natural abundance (%)	99.635	0.365	1.108
magnetic moment μ (μ_N)	0.57099	−0.4903	1.21211
magnetogyric ratio γ (10^7 radT^{-1} s^{-1})	1.9338	−2.712	6.7283
receptivity relative to that of ^{13}C	5.69	0.0219	1
nuclear quadrupole moment Q (10^{-28} m^2)	1.99×10^{-2}	0	0
line width factor l (10^{-59} m^4)[b]	2×10^{-3}		
NMR frequency Ξ (MHz)	7.226329	10.136783	25.145004
nuclear Overhauser enhancement (NOE)			
maximal proton-induced NOE factor		−4.93	1.99
reference standard (by substitution, for nitrogen)	neat liquid CH_3NO_2/CD_3NO_2		TMS

[a] Mills, I.; Cvitas, T.; Homann, K.; Kally, N.; Kuchitsu, K. *Quantities, Units and Symbols in Physical Chemistry*; Blackwell (for IUPAC): Oxford, 1993; pp 98−104. [b] $l = Q^2(2I + 3)/I^2(2I - 1)$.

Table 2. Reference Standards Used in Nitrogen NMR Spectroscopy for Solution and Solid State Work

CH_3NO_2 shifts/ppm in 0.30 M solution in different solvents[a]	δ (ppm)
in CCl_4	−7.1
in $CHCl_3$	−3.8
cf. neat liquid CH_3NO_2 (18.4 M)	0.0
in D_2O	2.0
in dmso	2.0

solid reference standards relative to neat liquid CH_3NO_2[b]	δ (ppm)
NH_4NO_3	−358.4
$(NH_4)_2SO_4$	−355.7
NH_4Cl	−341.0
NH_4NO_3	−5.0

[a] Witanowski, M.; Stefaniak, L.; Szymanski S.; Webb, G. A. *J. Magn. Reson.* **1977**, *28*, 217. [b] Ratcliffe, C. I.; Ripmeester, J. A.; Tse, J. S. *Chem. Phys. Lett.* **1983**, *99*, 177. Pestunovich, V. A.; Shterenberg, B. Z.; Lippmaa, E. T.; Myagi, M. Y.; Alla, M. A.; Tandura, S. N.; Boryshok, B. P.; Petukhov, L. P.; Voronkov, M. G. *Dokl. Akad. Nauk SSR* **1981**, *258*, 1410.

cal' standard. The spin-rotation determination of the nitrogen shielding (σ) in the isolated NH_3 molecule[14] provides an absolute scale for calculated values of the shielding.[15] $\sigma(Me^{15}NO_2)$ is −135.8 ppm, and shieldings for other molecules are given by $\sigma = -\delta - 135.8$.

Table 1 includes reference standards used in solid-state work. Note the large variation in NH_4^+ shift with different anions, particularly oxyanions, because of hydrogen bonding: 17 ppm from the nitrate to the chloride. The preferred standard is solid ammonium chloride[16] because of fast dipolar relaxation of $^{15}NH_4Cl$.[17]

C. ^{15}N Relaxation

^{15}N relaxation processes[2−7,18,19] are qualitatively similar to those of ^{13}C in similar environments, in >N═O and >C═O, for example, or $>NH_2$ and $>CH_2$, but the relative contributions of the various mechanisms differ. Dipolar relaxation by protons is less efficient for ^{15}N than for ^{13}C, since $|\gamma(^{15}N)|$ is only 40% of $\gamma(^{13}C)$ (Table 2). Other relaxation mechanisms, therefore, become more important for ^{15}N, particularly in nitrosyls, with no protons attached to nitrogen. Table 3 gives representative values of relaxation times and NOE factors, with examples of mechanisms.

The dipole−dipole (dd) relaxation rate for nitrogen bonded to n_H hydrogens is given by

$$1/T_{1dd} = (\mu_o/4\pi)^2 n_H(\gamma_H)^2(\gamma_H)^2\tau_c \qquad (1)$$

The relaxation time T_{1dd} is proportional to $(1 + \omega^2\tau_c^2)$, where ω is the resonance frequency and τ_c the effective ('correlation') time for the molecule to reorient itself in rotational motion. Equation 1 assumes 'extreme narrowing' conditions, of reasonable mobility, with $\omega^2\tau_c \ll 1$. The contribution to the relaxation rate per hydrogen at a distance of 10 pm, $5 \times 10^9\ \tau_c$, corresponds to T_{1dd} values of 15−80 s for nitrogen with one attached hydrogen in small- to medium-sized molecules in common solvents. Slower molecular tumbling may reach the Larmor precession frequency, below which spin−lattice relaxation is less effective as τ_c increases.[20] T_{1dd} falls to a minimum value near $\omega\tau_c = 1$ and then increases, depending on the field strength B_0, with concomitant changes in the NOE.

The decrease in T_{1dd} for longer correlation times is useful for biomolecules; thus, hemoglobin and vitamin B_{12} were studied in natural abundance of ^{15}N at 18.25 MHz (180 MHz for protons).[21] Working at higher fields can be detrimental since the T_{1dd} minima shift to smaller values of τ_c with increase in B_0. Wagging or spinning of a nitrosyl usefully reduces the effective correlation time.

The transverse (spin−spin) relaxation time T_2 decreases steadily with an increase in τ_c to a limiting value in the solid state determined by dipolar interactions; T_{2dd} has an additional τ_c-dependence which is independent of ω. Deuteration was used to improve ^{15}N resolution in hemoglobin studies through the γ^2 dependence of the dipolar relaxation rate.[22]

The microviscosity η', which is about one-sixth of the macroviscosity,[23] is important since the correlation time is proportional to η'/kT; also, T_2 depends on the microviscosity. Relaxation rates may be doubled, for smaller molecules, by use of more viscous solvents (dioxan, ethanol) or viscous additives (glycerol, polystyrene).[24] Cooling usefully increases the viscosity, the sensitivity, and correlation time.

Relaxation times may be quite long for ^{15}N in the absence of nearby hydrogen or alternative relaxation mechanisms: neat liquid nitrobenzene and benzonitrile have $T_1 > 400$ s, cf. 140 s for aqueous nitrate (Table 3).[25] Nitrogen exposed to the solvent, as in a

Table 3. Representative ^{15}N Relaxation Times (T_1), NOE Factors (η_{obs}), Correlation Times (τ_c) ,and Relaxation Mechanisms

compound[a]	T_1 (s)	B_o (T)	η_{obs}	τ_c (ps)[b]	mechanism[c]	ref
$PhNO_2$ (l)	450	1.41	−1.8	($\tau_q = 10$)	sr, dd	25
	170	7.42	−0.6	4	sa, sr	30
PhCN (l)	420	1.41	−1.6	($\tau_q = 7.5$)	dd, sr, e	25
NH_4NO_3 (1:1 w/w in H_2O)	140	1.41	−0.9		sr	25
CH_3CN (l)	90	6.34				25
with 5×10^{-4} M [$Gd(acac)_3$]	53	6.34			e	25
pyridine (l)	85	6.34	−0.4		sa, dd, sr	25
with 5×10^{-2} M [$Cr(acac)_3$]	3.7				e	25
^{n}BuNH$_2$	70	6.34	−3.9		dd	25
pyrrolidine (l) >NH	58	6.34	−4.6	4	dd	25
trans-PhN=NPh (2.7 M in $CDCl_3$)	56	2.11			sr, dd, sa	27
pyrrole (l) aromatic >NH	40	6.34	−4.3	5	dd	26
NH_4NO_3 (1:1 w/w in H_2O)	37	1.41	−4.93		dd	25
^{n}BuONO (l)	24	2.11			sr(int)	27
$NaNO_2$ (0.7:1 w/w in H_2O)	23	1.41	−0.4		sr,sa	25
$NaNO_2$ (1.1 M in D_2O)	19.0	4.7				
	17.5	9.4				
KCN (1 M in 1:1 H_2O/D_2O, pH 12.5)	21	1.41	0		sa, sr	29
	14.5	4.23	0		sa, sr	29
CH_3CONH_2 (5.3 M in H_2O)	14.2	1.41	−5.1	7.5	dd	26
N_2 (l, 77 K)	15	0.70		($\tau_{sr} = 0.2$)	sr	*e*
N_2 (l, 126 K)	1.5	1.02		($\tau_{sr} = 1$)	sr	*e*
$TPPH_2^{2+}$	1.9	4.23	−4.93		dd	*f*
ZnTPP[c] (6×10^{-3} M in $CHCl_3$)	56	4.23	0		e, etc	*f*
lysozyme (9.4×10^{-3} M in 0.1 M citrate, pH 5)	4.23				*g*	
−C(O)−NH−	0.16		−0.5	5000	dd	
$>NH_2^+$	0.33		−3.5	3500	dd	
solids						
NH_4Cl	4	4.70		14	dd	*h*
TPP[d] (180 K) aromatic >NH	0.67	1.41	0.7		dd, pe	32
aromatic −N=	0.05	1.41	0.1		sa, dd, pe	32

[a] Measurements were made at ambient temperatures (300 ± 3 K) if no other temperature is given. [b] τ_c values are in picoseconds (10^{-12} s). [c] Relaxation mechanisms are given in order of decrease in their contribution: dd = dipole−dipole (intra- or intermolecular), sr = spin-rotation, (int) = internal, sa = shielding anisotropy, e = electron−nuclear, sc = scalar coupling, pe = proton exchange. [d] TPP is *meso*-tetraphenylporphin. [e] Ishol, L. M.; Scott, T. A.; Goldblatt, M. *J. Magn. Reson.* **1976**, *23*, 313. Krynicki, K.; Rahkaa, E. J.; Powles, J. G. *Mol. Phys.* **1975**, *29*, 539. [f] Gust, D.; Roberts, J. D. *J. Am. Chem. Soc.* **1977**, *99*, 3637. [g] Gust, D.; Moon, R. B.; Roberts, J. D. *Proc. Natl. Acad. Sci.* **1975**, *72*, 4696. Dubin, S. B.; Clark, B. W.; Benedek, G. B. *J. Chem. Phys.* **1971**, *54*, 5158. [h] Hunter, B. K.; Brown, R. J. C. *J. Magn. Reson.* 1982, **46**, 227.

bent nitrosyl, can experience intermolecular dipolar relaxation in which T_{1dd} is directly proportional to the distance of closest approach of hydrogen.

Electron−nuclear relaxation is usually present with metal nitrosyls because of paramagnetic contamination to which basic nitrogen is very sensitive: rigorous purification is needed in measuring nitrogen relaxation times.[26] Paramagnetic additives are useful for quantitative studies, quenching dipolar relaxation, and the NOE (with susceptibility corrections for accurate shift measurement). Carbonyl groups in [$Cr(acac)_3$] can form hydrogen bonds with NH groups. [$Gd(acac)_3$] interacts with basic nitrogen and can be used for spin labeling. Effects of dissolved oxygen are small.

The spin-rotation (sr) mechanism, increasing as kT, relaxes ^{15}N in freely rotating nitrosyl, nitro, or nitrito[10,27] groups (Table 4).

Shielding anisotropy ($\Delta\sigma$) relaxation of ^{15}N is important for bent or linear nitrosyls, as for −C≡N and −N≡N ligands,[28] CN^- [29] and NC^- ions, planar groups (nitro or nitrate), or azines (Table 4). This relaxation is faster in a more viscous solvent or with viscous additives to increase the correlation time. Cooling increases the sensitivity also, increasingly at higher fields, since the rate is proportional to $(\Delta\sigma)^2$ and to B_o^2. Table 4 shows the increase in relaxation rate with increase in the applied field for CN^- and nitrobenzene,[30] and values of $\Delta\sigma$ are discussed in section IV.

Commonly several mechanisms (sa, dd, and sr) are operative. ^{15}N is relaxed also by scalar coupling to (quadrupolar) ^{16}O in nitrosyls, as to ^{14}N in $^{14}N^{15}N$ gas.[31] Hydrogen-bonded ^{15}N is relaxed by proton exchange (pe), also in the solid state, as in *meso*-tetraphenylporphin ($TPPH_2$), in which two hydrogens exchange between the central four nitrogens: the unprotonated nitrogen relaxes by the sa mechanism, by dipolar interaction with the protons on the other nitrogens, and through proton exchange.[32]

D. ^{15}N NOE Factors

If ^{15}N is wholly relaxed by $^{15}N/^1H$ dipolar interactions, broad-band proton decoupling will give a maximal NOE factor[33] η (note that the symbol η is used also for the viscosity)

$$\eta_{max} = \gamma(^1H)/2\gamma(^{15}N) = -4.93 \qquad (2)$$

Since $\gamma(^{15}N)$ is negative, the signal diminishes then changes sign. The maximal value is an improvement on the ^{13}C value of 2.99, and collapse of multiplets may increase the signal height. The observed NOE factor depends on the proportion of the relaxation

Table 4. Examples of ^{14}N Line Widths ($W_{1/2}$), Relaxation Times (T_q), Nuclear Quadrupole Coupling Constants (χ), and Correlation Times (τ_q)

sample[a]	$W_{1/2}$[b] (Hz)	T_q (ms)	χ (MHz)	η[c] (cP)	τ_q[d] (ps)	ref
		four-coordinate nitrogen				
Me_4NBr (1 M aq, 316 K)	0.1	0^4				55
NF_4AsF_6 (HF)	3.0					49
NH_4Cl (1 M aq, 316 K)		1600		1.08	5.9	55[e]
NH_4Cl, ND_4Cl (s, 295 K)		700−800	0.016		20	17[e]
$Na[Co(NH_3)_2(NO_2)_4]$ (aq)	170		2.09			83
$[Co(NH_3)_6Cl_3$ (aq)	370		3.62		10.3	83
$[Co(NH_3)_6](ClO_4)_3$ (0.24−0.5 M/dmso)	0.29	3.3		20	104	83
		six-coordinate nitrogen (interstitial)				
$[Rh_6(m_6\text{-}N)(CO)_{15}]^-$(acetone-$d_6$)	20					56
		linear two-coordinate nitrogen				
N*N*O (15 atm in hexane)	0.45	2960	0.238		20	59
MeNC (l)	0.26	1220	0.27	0.35	30	50
NO_2AsF_6(HF)	5					49
PdCNBu^t complexes($CDCl_3$)	4−12	30−80				82
NaN_3 (1 M aq) N*M*N$^-$		29.3	1.03			57
$[(\eta^5\text{-}C_5H_5)Mo(CO)_2(NO)](CH_3CN)$	30					79
$[Mo(NO)(S_2CNMe_2)_3](CH_2Cl_2)$	40					78
$[Mo(NS)(S_2CNMe_2)_3](CH_2Cl_2)$	150					81
		terminal (one-coordinate) nitrogen				
N_2O (15 atm in hexane) *N*NO		280	0.792			59
N_2 (l, 126 K)		18.5	5.39			28
N_2 (l, 77 K)		1.7	0.074	0.2		28
$^{14}N^{15}N$ (g, 294 K)	15.3					31
NaN_3 (1 M aq) *N*N*N*$^-$		7.4	1.79			57
MeCN (1% v/v in hexane)	53.5		3.74	0.29	0.82	75
MeCN (l)	78		0.34	0.67		75
$NO^+AsF_6^-$(HF)	95					49
MeSCN(l)		2.0	3.75	0.72	2.4	62
NC−C≡C−CN (5 M in tol-d_8)	189	1.7	4.14	0.45	2.36	81
NC−C≡C−CN (infinite dilution in hexane)	244		4.14	0.30	4.75	28
NC−C≡C−CN (infinite dilution in hexane) (l)	394			0.60		28
$K_3[Co(CN)_6]$ (aq)	570		3.62		16.0	
		planar three-coordinate nitrogen				
$NaNO_3$ (s)		10^5	0.745			58
$NaNO_3$ (1 M aq, 295 K)		85			$t_\perp = 1.43$	58
$EtONO_2$ (l)		45	0.9		2	62
$MeNO_2$ (l)		22	1.7	0.6	1.03	62,63
$(NOF_2)AsF_6$(HF)	18					49
pyridine *N*-oxide (0.2 M, CCl_4)	28.3	11.2	1.1		3.4, 11.9, 2.9	73
$PhNO_2$ (1:1 v/v, hexane)		6.2	1.426	1.83	3.6, 11, 4.4	65
$PhNO_2$ (l)		3.2			7.0, 2.1, 6.3	58
PhN=*N*(O)Ph (l, 284 K)	700		1.4		10	58
		pyramidal nitrogen				
$MeNH_2$ (l)	30		3.98	0.18	0.55	69
Me_2NH (l)	125		5.05	0.17	1.0	69
Me_3N (l)	100		5.2	0.16	0.8	69
NF_3 (l, 108 K)	318	1	7.07		1.35	71
EtONO (l)		5.2	3.8		0.9	62
pyridine (l)		1.65	4.58	0.89	1.95	64
C_5H_5ONO (l)		1.6			3.0	62
$Na[Co(NH_3)_2(ONO)_4]$ (aq)	700		4.25		14.25	83

[a] Measurements were made at ambient temperatures (300 ± 3 K) if no other temperature is given. [b] Observed line widths may contain unresolved couplings. [c] Viscosity. [d] τ_q values are in ps (10^{-12} s); compare the values measured in ^{15}N resonance (Table 4). Three values correspond to $\tau_{x,y,z}$: the *x* direction is the axial bond to nitrogen, and the *y* direction is in the molecular plane. [e] Cooke, D. F.; Jeffrey, K. R. *J. Magn. Reson.* **1975**, *18*, 455.

that is mediated by ^{15}N/^{1}H dipolar interactions

$$\eta_{obs} = (I - I_0)/I_0 = -4.93\,(T_1)_{obs}/T_{1dd} \qquad (3)$$

Although the NOE is sizable for nitrogen with one or more attached protons, the NOE is small and detrimental for nitrogen with few nearby protons, as in metal nitrosyls. The signal may then diminish, with more efficient modes of relaxation taking over,[34] vanishing when 20% of the relaxation is dipolar ($I =$ 0, $\eta_{obs} = -1$). Disadvantageous NOE may be removed by gated decoupling or by paramagnetic additives to promote electron−nuclear relaxation.

E. ^{15}N Sensitivity Enhancement

^{15}N sensitivity is enhanced by use of larger samples, higher fields, lower temperatures, proton decoupling, and the NOE, if favorable. If the nitrogen is coupled to protons or other more NMR-sensitive nuclei, pulse sequences can be used to transfer their polarization

to nitrogen. The $\gamma(^1H)/\gamma(^{15}N)$ ratio gives a 10-fold enhancement, and the faster proton relaxation allows faster pulsing.

Spin−spin coupling to protons, if resolvable, can be used for magnetization transfer in liquid samples, by methods such as *J*-cross-polarization (JCP), selective polarization transfer (SPT), insensitive nuclei enhanced by polarization transfer (INEPT), distortionless enhancement by PT (DEPT), and variants,[3,7,35] allowing measurements in natural abundance of ^{15}N in >NH systems, or using longer-range couplings in delocalized systems.[36,37] Such methods are used to determine coupling constants and their signs, to establish connectivities, distinguishing different nitrogen environments, to investigate relaxation processes, and to measure relaxation times.

Multiple quantum methods involving double magnetization transfer $^1H \rightarrow {}^{15}N \rightarrow {}^1H$ increase ^{15}N sensitivity by detecting ^{15}N in proton spectra and correlate ^1H and ^{15}N shifts in 2D spectra through spin−spin coupling pathways.[38] $^{15}N \rightarrow {}^1H$ polarization transfer is used in 2D spectroscopy to assign ^{15}N signals in biomolecules,[39] while 2D, 3D, and 4D correlation spectroscopy (COSY) experiments can correlate ^{15}N, ^{13}C, and proton resonances, particularly in biosystems.[40,41] Magnetization may be transferred to ^{15}N from from ^2D, ^{19}F, or ^{31}P; with ^2D, fast quadrupolar relaxation outweighs the small magnetogyric ratio compared with the proton. In solid-state work (section IV) cross-polarization (CP) is used to transfer magnetization to ^{15}N via dipolar couplings.

F. Isotope Effects

Primary isotope effects on nitrogen shifts are negligible, and ^{14}N and ^{15}N shifts are interchangeable. Bloch-Siegert shifts, arising from the negative magnetogyric ratio of ^{15}N, are detectable in double resonance experiments, and corrections may be needed in the determination of accurate values of chemical shifts by homonuclear decoupling experiments.[42]

Nearest-neighbor isotope effects may be observed in accurate work. A heavier isotopic substituent normally increases the nitrogen shielding, and there is some additivity for multiple substitution. Deuteration increases the nitrogen shielding by about 0.65 ppm per hydrogen replaced in NH_3, 0.3 ppm in NH_4^+, and 0.5−0.7 ppm in pyridinium ion, amines, or amides.[43] Equilibrium isotope effects can be observed if deuteration perturbs tautomeric or hydrogen-bonding equilibria.[44] Effects of replacing an ^{16}O neighbor by ^{18}O, about 0.15 ppm per oxygen in nitrite ion or 0.06 ppm in nitrate, can be useful in mechanistic studies, and ^{18}O labels can be monitored by ^{15}N NMR, as in the bacterial oxidation of ammonia to nitrite or of nitrite to nitrate.[45]

Equilibrium isotope effects, arising from mass-dependence of equilibria, may be larger. The five-coordinate complex $[RuCl(NO)_2(PPh_3)_2]^+$, with one bent and one linear nitrosyl in the solid state, is bent ↔ linear fluxional in solution, and the 50% enriched compound gives a doubled nitrogen line,[46] since linear ^{15}NO is slightly favored in the $(^{14}NO)(^{15}NO)$ molecule (raising the shielding slightly). This isotope effect is observable because of large differences in stretching frequency and nitrogen shift in linear and bent nitrosyls, effects of the lone pair on the bent nitrogen. The temperature-dependence of the equilibrium isotope effect and the ^{15}N shifts in solution and the solid (described in section VI) show that a trigonal-bipyramidal structure with two linear nitrosyls probably contributes to the fluxions in solution.[46,101]

G. Medium Effects

Because of the importance of nonbonding electrons to nuclear magnetic shielding and spin−spin coupling, NMR properties of nitrogen carrying a lone pair are very sensitive to changes of solvent, concentration, counterion, or pH; thus, they are a useful probe of inter- and intramolecular influences and equilibria. Medium effects on nitrogen shielding may be large if hydrogen-bonding or acid−base interactions are present: the shifts are in the same direction as protonation shifts but smaller (Table 2). Hydrogen bonding to a lone pair on nitrogen decreases the nitrogen shielding in saturated groups such as ammonia and alkylamines,[47,48] while hydrogen bonding to nitrogen increases the shielding of that nitrogen.[49] Hydrogen-bonded systems, therefore, show complex behavior, including proton exchange. Table 2 demonstrates the sensitivity of the nitrogen shielding to distortions in the ammonium ion by hydrogen bonding in the crystal lattice, with increases of 14.7 ppm from the chloride to the sulfate and 2.7 ppm from the sulfate to the nitrate.

In the nitrosyl group the sensitivity of NMR properties to lone pair or π electron density on the nitrogen means that they are sensitive to the changes of solvent, concentration, pH, or counterion to which nonbonding electrons respond. Nitrogen NMR spectroscopy is thus a useful probe of inter- and intramolecular influences and equilibria.

Similarly, hydrogen bonding to a lone pair on nitrogen in a p-bonded system increases the nitrogen shielding. Again, the shifts are in the same direction as protonation shifts but smaller in magnitude. Medium effects when the nitrogen carries p but not lone pair electrons are illustrated by the 9 ppm range shown in Table 2 for the nitrogen shift in nitromethane in different solvents.

Medium effects are observable also in spin−spin couplings to nitrogen, because of their sensitivity to the presence of lone pairs.

H. ^{14}N Line Widths: Quadrupolar Broadening

Although ^{14}N gave way to ^{15}N NMR spectroscopy, newer techniques can turn ^{14}N quadrupolar interactions to advantage. Fast relaxation allows faster pulsing, spreading nitrogen spectra over a large range;[50,51] wide variation in ^{14}N line widths must be taken into account in quantitative work.[52] High-resolution work is possible if the ^{14}N mobility and local electronic symmetry are both high. Lines are sharpened by warming the sample or using more mobile solvents.

The (Lorentzian) line width at half-height $W_{1/2}$ is proportional to the relaxation rate $1/T_q$ and to the square of the nuclear quadrupole coupling constant

χ. For mobile species (extreme narrowing) with $\omega^2\tau_q \ll 1$ (angular frequency ω, correlation time τ_q), the line width is given by

$$\pi W_{1/2} = 1/T_q = \frac{3}{8}\chi^2(1 + \eta^2/3)\tau_q \qquad (4)$$

where T_q ($= T_1 = T_2$) is the quadrupolar relaxation time, $\chi = e^2qQ/\hbar$ in radians, $\eta = (q_x - q_y)/q_z = eq$, the asymmetry parameter, more precisely eq_z, where $|q_z| \geq |q_x| \geq |q_y|$) is the electric field gradient (efg) at the nucleus

Relaxation of ^{14}N is usually quadrupolar since the quadrupole is relatively small and the rate depends on χ^{-2}. Line widths are very sensitive to the magnitude of χ but less sensitive to the asymmetry parameter which is ≤ 1 by definition. χ values are obtained from NQR spectroscopy of solids, from microwave spectroscopy of gases, and by NMR methods.[53]

The ^{14}N electric field gradient depends on the symmetry of the valence p electrons, as distorted by collision. In bent paramagnetic nitrosyls, ^{14}N relaxation may be quadrupolar because of the nitrogen anisotropy while the nitrogen shows contact shifts, as observed for cyano complexes $K_3[M(CN)_6]$ (M = Cr, Mn, Fe).[54]

Table 4 gives representative ^{14}N line widths, relaxation times, NQCC values χ, and correlation times τ_q. Lines are quite sharp ($\chi \leq 1$ MHz) in NH_4^+,[51] as for R_4N^+ species,[55] or interstitial nitrogen in cobalt and rhodium clusters $[M_6N(CO)_{15}]^-$;[56] or for central nitrogen in NO_2^+,[6a] N_3^-,[57] or NO_3^-,[58] all highly mobile in solution; and also if the substituents on nitrogen have similar electronegativity, as in linear N*N*O[59] and isonitriles RNC.[60,61] Broader lines are observed for $EtONO_2$, $MeNO_2$,[62,63] or NOF_2^+,[28] broader still for bulkier molecules such as pyridine *N*-oxide,[64] Ph-NO_2,[65] or PhN=N(O)Ph.[66]

In bent nitrosyls the efg and line width are greatly increased by the nitrogen lone pair, as also in organic isocyanates,[67] nitrites,[75] and pyridine,[68] and for pyramidal nitrogen in tertiary amines.[69−72] The lone pair s-electronic component is close to the nucleus, particularly with electronegative substituents. On terminal nitrogen a lone pair is less effective in line-broadening because of the axial symmetry, but electronegative substituents broaden the lines, as from N_2[42,47] to RCN[73−77] and to NO^+.[28] In liquid N_2O the nitrogen line widths are in the ratio of the NQCCs determined by microwave spectroscopy in the gas phase.[60] NQCC values fall on protonation or coordination of the nitrogen and with delocalization of a lone pair in conjugated systems.

Ligands in metal complexes can be studied by ^{14}N NMR if the molecules are not too bulky or associated. Linear NO or NS coligands in molybdenum dialkyldithiocarbamato complexes give sharp ^{14}N lines,[78] and $^{95}Mo-^{14}N$ couplings were resolved for η^5-C_5H_5 complexes with NO and CO ligands, despite the ^{95}Mo and ^{14}N quadrupoles.[79] ^{14}N lines are reasonably sharp for the imido (nitrene) ligand =NR in *trans*-[WF_4(NMe)L] complexes,[80] even with bulky R groups such as $SiMe_3$ (helped by internal mobility) in Ta, W, and Os complexes,[81] similarly Bu^t in $PdCNBu^t$ complexes.[82] ^{14}N lines are broader for ligating nitrogen with bulky (e.g., phosphine) coligands and with greater differences in electronegativity of the nearest neighbors, as in ammine and diamine complexes of cobalt.[83]

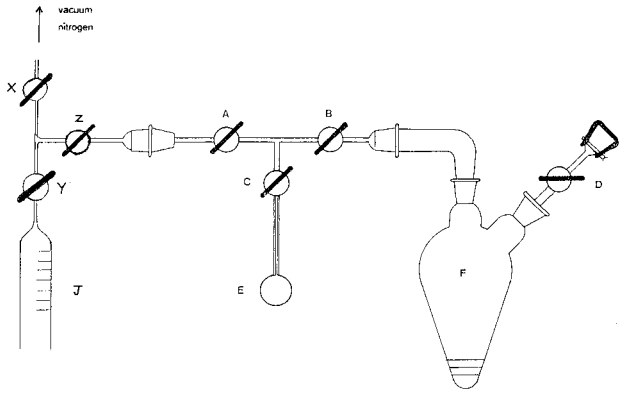

Figure 1. Apparatus for the preparation of ^{15}NO from $Na^{15}NO_2$.

^{14}N line widths may be halved by using more mobile solvents (ether instead of chloroform, acetone instead of water) or super- or near-critical fluids: $^{14}N^{14}N$ and $^{14}N^{17}O$ couplings were measured in liquid N_2O,[84] and highly mobile fluoro compounds are readily measured.[28] Warming may help as the viscosity decreases exponentially with increase in temperature.

II. Preparation of ^{15}N-Enriched Metal Nitrosyls (L. F. Larkworthy)

Many of the metal nitrosyls studied by ^{15}NMR spectroscopy, as described here, were prepared first from unlabeled nitric oxide. This was generated by reaction of aqueous sodium nitrite and acidified iron(II) sulfate to give the brown-ring complex $[FeNO(H_2O)_5]_2^{2+}$ which readily decomposes to give NO gas[85]

$$2NaNO_2 + 2FeSO_4 + 3H_2SO_4 = Fe_2(SO_4)_3 + 2NaHSO_4 + 2H_2O + 2NO \qquad (5)$$

An all-glass apparatus was used to generate and store the NO, as in Figure 1. From ca. 200 mL of NO, gram quantities of metal nitrosyls were prepared, avoiding the expense and perhaps erratic supply of nitric oxide cylinders. For example, the complex [Co(NO)(phsal)$_2$] (Figure 3) was prepared by mixing solutions of *N*-phenylsalicylaldimine and cobalt(II) acetate tetrahydrate in dimethylformamide under an atmosphere of NO, connected to a gas buret (J) so that the uptake of NO could be measured; Co(II) and NO combine in equimolar amounts. This complex was also prepared by reaction of NO with previously isolated $[Co^{II}(phsal)_2]$.[86]

Experimental procedures were first tested with natural abundance sodium nitrite. For economy of $Na^{15}NO_2$, the ^{15}N-labeled gas was generated from a layered mixture of small quantities of solid $Na^{15}NO_2$, $FeSO_4 \cdot 7H_2O$, and NaBr by the reaction[87]

$$Na^{15}NO_2 + FeSO_4 + NaBr + H_2O \rightarrow {}^{15}NO + Fe_2(SO_4)_3 + NaBr + H_2O \qquad (6)$$

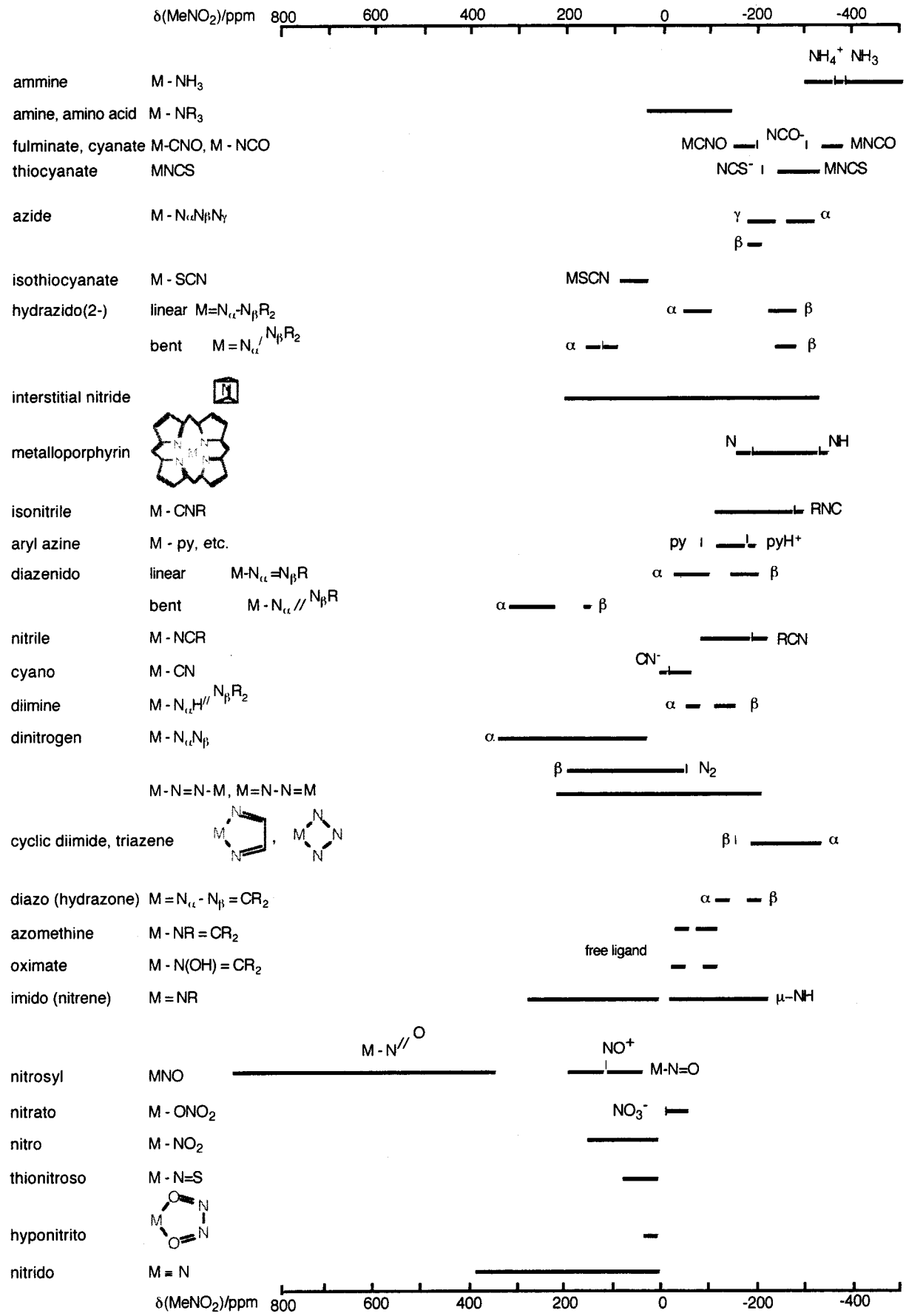

Figure 2. Coordination shifts of nitrogen in metal complexes.

To initiate the reaction, a little water was added to dissolve the reactants.

The apparatus in Figure 1 consists of a small bulb (E) of about 1 cm diameter and spring-loaded stop-

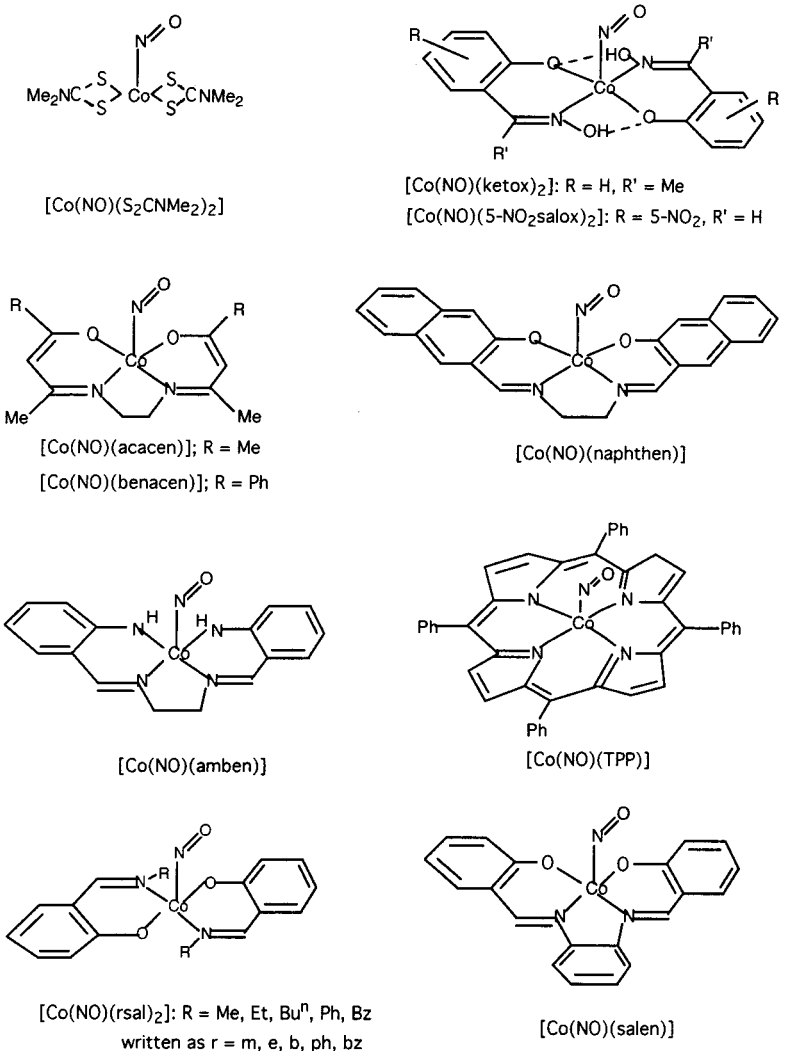

Figure 3. Structures of complexes with a bent apical nitrosyl ligand for which ^{15}NO and ^{59}Co shifts were measured in solution and ^{15}N shielding tensors were measured in the solid state.

cocks (A, B, and C) with narrow tubing to lessen the dead-space, connected to a two-necked 100 mL pear-shaped flask (F), equipped with a stopcock (D) and a subaseal on the sidearm, and (via stopcock Z) to a gas buret (J) for storing ^{15}NO.

In a typical experiment, iron(II) sulfate heptahydrate (0.900 g, 3.3 mmol), anhydrous sodium bromide (0.425 g, 4.1 mmol), and ^{15}N-labeled sodium nitrite (0.200 g, 2.9 mmol) were layered in this order in the bottom of flask F which contained a small stirring bar. Air was pumped out and nitrogen admitted. The solids were cooled in liquid nitrogen, and deoxygenated water (1.0 mL) was injected onto the solids by syringe with a long needle passed through the subaseal and stopcock D. The water froze, and no reaction occurred. The needle was withdrawn and D closed. Flask F was then evacuated with A, B, and C open. These stopcocks were then closed, the coolant removed, and the flask allowed to warm.

Once the ice melted, stirring was started to aid the release of the ^{15}NO under reduced pressure in flask F. The color of the solution changed to brown, with vigorous effervescence. After the reaction was complete, the ^{15}NO pressure in F would have been equivalent to about 50 cm of mercury. Some ^{15}NO was drawn into buret J (previously filled with mercury) by opening the appropriate stopcocks carefully, but much gas remained in F. This was condensed in E with a liquid nitrogen trap and then allowed to evaporate into J with B closed.

Volumes of ^{15}NO ranging from 52 to 63 mL (corrected to STP) were obtained from 0.2 g of $Na^{15}NO_2$. Although Brauer[88] specifies a molar deficiency of iron(II) sulfate with respect to the nitrite, we found an excess of the reducing salt to improve the yield of ^{15}NO.

A. Preparation of ^{15}N-Enriched Metal Nitrosyl

About 15 mL of ^{15}NO gas was used to give a 5% excess and ensure complete reaction of the paramagnetic cobalt(II) salt. The gas buret was attached to an evacuated reaction flask containing the other reactants and the appropriate volume of ^{15}NO transferred in. The nitrosylation is irreversible, and reaction under reduced pressure goes to completion in good yield.

In the preparation of [Co(^{15}NO)phsal$_2$], for example, cobalt(II) acetate tetrahydrate (0.17 g, 0.68 mmol) in methanol (3 mL) was mixed with *N*-phenylsalicylaldimine (0.27 g, 1.37 mmol) in methanol (2 mL) in an

atmosphere of ^{15}NO (20 mL at room temperature and pressure, 15.4 mL (0.685 mmol) at STP). The dark green [Co(^{15}NO)phsal$_2$] was obtained in 45% yield (0.144 g). Thus, 0.2 g of $Na^{15}NO_2$ gave sufficient ^{15}NO to make samples of at least four metal nitrosyls for measurements of the ^{15}N shielding tensors in the solid state.

III. Patterns of Nitrogen Shifts in Metal Nitrosyls and Related Compounds

Shift ranges reported for metal complexes with ligating nitrogen are given in Figure 2, with free ligand shifts for comparison.

Clearly, the nitrogen resonates at very high frequency (low field) in bent nitrosyls and rather high frequency in linear nitrosyls. The NMR shift in diamagnetic compounds is mediated by the (magnetic dipole allowed) $\sigma \leftrightarrow \pi$ (here p − p) circulations of the observed nucleus's valence elections in the magnetic field. Particularly effective, because of their low excitation energies ΔE, are $n_N-\pi^*$ circulations in the nitroso/nitrosyl group. n_N refers to nonbonding electrons with p character (sp or sp^2) on nitrogen in high-lying orbitals, while π^*(N═O) (unoccupied) orbitals are low-lying because of the high electronegativity of oxygen and nitrogen.

An approximate equation for the paramagnetic term σ_p

$$\sigma_p \approx -\frac{\mu_o}{4\pi}\frac{e^2}{2m_e^2}\langle r^{-3}\rangle_{2p}\frac{\langle 0|L^2|0\rangle}{\Delta E[n(N)\rightarrow \pi^*(NO)]} \quad (7)$$

shows the three factors determining the shifts. (1) A radial term $\langle r^{-3}\rangle_{2p}$, the average of r^{-3} for an electron in a 2p orbital on nitrogen. The nitrogen shift range is double that for carbon because the radial term[88] is twice as large for atomic nitrogen (2.46 au) as for carbon (1.23 au) (again, an electronegativity effect). (2) The angular momentum term in L^2, representing the circulation of electronic charge in the magnetic field when the valence shell p,d orbitals are asymmetric. This circulation reinforces the applied field and so opposes the diamagnetic circulation, which is fully realized only in the free atom or around the axis of a linear molecule. Charge asymmetry is large for two-coordinate nitrogen carrying a lone pair, as in the nitrosyl group, and very large when −N═O is bent. (3) The effective excitation energy ΔE for the paramagnetic $\sigma \leftrightarrow \pi$ circulation, as the magnetic field mixes appropriate excited states into the ground state. This qualitative picture is described more rigorously in later sections.

Excitation energies vary more widely for nitrogen than for carbon because nitrogen can carry a lone pair and LUMOs are lower than for carbon, on electronegativity grounds. The frontier orbitals are those involving charge rotation, $n(N)\rightarrow\pi^*$ or $\sigma \leftrightarrow \pi^*$ but not $\pi \rightarrow \pi^*$ or $\sigma \leftrightarrow \pi^*$ (in the same bond). Magnetic-dipole-allowed excitations, normally forbidden in the electronic spectrum, are weakly allowed in $n_N \rightarrow \pi^*$ excitations because of their s → p component and produce the long wavelength bands which give N_2O_3 and organic nitroso compounds their blue color. Interaction of the −N═O chromophore with the d-orbital system produces the great variety of colors and nitrogen shifts of transition-metal nitrosyls. Equation 7 shows that the chemical shift (deshielding) is greater the closer the paramagnetic circulation to the nucleus (the more electronegative the substituents), the smaller the energy ΔE of the virtual excitation, and the greater the imbalance of charge in the valence shell, giving the much larger deshieldings for bent than for linear nitrosyl or nitroso compounds.

The importance of the $n(N) \rightarrow \pi^*$ excitation in nitrogen shielding is well-known.[1−3] In main-group compounds with a bent nitroso or nitrosyl group the nitrogen is progressively deshielded (the NMR line moves to higher frequencies) as the $n(N) \rightarrow \pi^*$ absorption moves to longer wavelengths,[89] from NOF (colorless) to RONO or R_2NNO (pale yellow) to NOCl (red-brown), NOBr, RSNO (red), and RNO (deep blue, δ = 594 ppm for Bu^{t}NO[90]). Deshieldings up to 800 ppm are reported for bent compared with linear metal nitrosyls,[91] and smaller MNO angles give larger deshieldings.[90] ^{14}N NMR was used early on to show that N_2O_3 has the O_2NNO structure rather than Sidgwick's ONONO structure;[92] ^{15}N NMR was used to differentiate the linear and bent geometry of diazenido[93] and nitrosyl ligands.[94]

Reactions in which a d-electron pair moves onto ligating nitrogen, allowing the metal to accept an incoming ligand and the nitrogen to coordinate a Lewis acid, are readily monitored by nitrogen NMR. Motions of a bent nitrosyl in the solid state, such as swinging or spinning,[95] can be inferred from changes in the nitrogen shielding tensor[96] as described in section IV.

A. Nitrogen NMR Criteria of Structure

Nitrogen is deshielded with decrease in the bond angle in groups which may be linear or bent, and the deshielding is greater, the greater the deshielding in the linear group; thus, nitrosyl nitrogen is more strongly deshielded on bending than azido −N*N*N or imido ═NR nitrogen.

As for nitrosyl bridging, in groups which may be pyramidal at nitrogen carrying a lone pair, or flatter, with π-delocalization, the nitrogen is deshielded the flatter the group (as noted early on in substituted anilines) since planarity allows $\pi \leftrightarrow \sigma$ paramagnetic circulations of lower energy than $n_N \rightarrow \sigma^*$ circulations in the pyramidal group. In the planar hydrazido(2−) ligand M═N−NH_2, the −NH_2 nitrogen shielding is lower than for hydrazines and comparable with amide shifts.[97]

Protonation and deprotonation shifts have diagnostic value in structural studies. Hydrogen bonding to a lone pair on nitrogen leads to smaller shifts in the same sense as a protonation shift, while hydrogen bonding of attached hydrogen gives nitrogen shifts in the opposite sense. Information on tautomeric and other acid−base systems involving nitrogen is thus available from the nitrogen shifts (and couplings), ^{14}N line widths, and ^{15}N NOE.

B. Coordination Shifts[2]

Changes in shift on coordination to a metal, shown graphically in Figure 2, may be of either sign and depend on the following. (1) The degree of reorganization of the electronic disposition in the ligand, which is NO^+ in linear nitrosyls, NO^- in bent nitrosyls; thus, coordination shifts are small for ammines and may be large for nitrosyls. (2) Donor−acceptor properties of the ligand: for π-acceptor ligands such as NO^+, NO^-, CO, or N_2, the $n(\sigma)$ HOMO is stabilized by coordination and the π^*NO LUMO destabilized by back-bonding, tending to increase $\Delta E(n \rightarrow \pi^*)$ and therefore the nitrogen shielding, although $\sigma \leftrightarrow \pi$ circulations involving the metal tend to lower the shielding. (3) The metal: coordination shifts are usually larger for transition metals with low-lying *d* orbitals than for non-transition metals. The importance of ligand-field splittings is shown by the periodic dependence of the coordination shift on the transition metal and by trans effects.[98] For π-acceptor ligands such as −N═O, the shielding increases across the transition series and down the group, in contrast to π-donors such as the nitrido ligand ≡N. The metal's oxidation state and the charge on the complex are significant also, since increased availability of electronic charge deshields π-acceptor ligands. (4) The symmetry of the coordination sphere and the ligand field. (5) Coligands: polyhapto arene ligands and π-donor *trans*-ligands tend to decrease the shielding of π-acceptor coligands. (6) Ligand hapticity: in NO^+ or CO the shielding decreases from terminal to bridging ligands, as linear geometry MNO/MCO is replaced by planar M_2NO or M_2CO. (7) The degree of bending of ligating (two-coordinate) nitrogen: the shielding decreases sharply from the linear to the bent ligator, as in diazenido, diazene, and hydrazido complexes, as well as nitrosyls.

Ranges of coordination shifts may be large if there are low-lying excited states, as variations in a small excitation energy have a large effect.

Other back-bonding ligands (phosphines, phosphites, PF_3) show similar periodicities to linear NO and CO; phosphines usually show deshielding of ^{31}P on coordination. Ligands showing increased shielding on coordination include H^-, ^{13}C in σ- or π-donor organo groups, CN^-, and nitrogen in amines, azide, NCO^-, or NCS^- ions.

C. Ligand Field Effects in the Nitrogen and Metal Shielding

In its ability to bend, the nitrosyl ligand stands out from the related (isoelectronic) ligands CO and N_2 which are constrained to linearity. When the nitrosyl ligand bends, a lone pair develops on the ligating nitrogen, and the strongly bent ligand is usefully viewed as NO^- attached to (low-spin) cobalt(III), in the compounds shown in Figure 3.

The nitrosyl ligand's ability to bend has been explained in terms of the similarity of the energies of the *n*(N) HOMO and the π^* LUMO in the nitrosyl ligand to those of the (d−d) ligand-field orbitals.[99] The low-lying π^*(NO) orbitals are excellent d-electron acceptors, and $d\sigma^*$(M−N) electron density in $[MNO]^8$ complexes can be stabilized as a lone pair on nitrogen in the bent ligand.

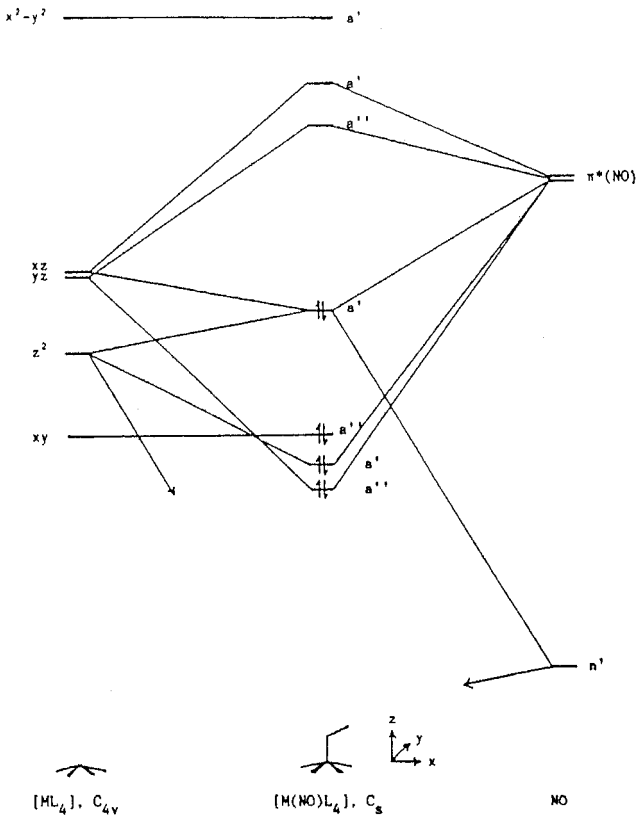

Figure 4. Scheme showing interactions of n′(N), π^*(NO), and ligand-field orbitals in a square-pyramidal complex of cobalt with bent apical nitrosyl. (Reprinted with permission from ref 91. Copyright 1987 American Chemical Society.)

The combination of the ligand-field theory of metal nitrosyl bending[99] with the shielding theory which relates the nitrogen shift to the degree of bending suggested a link between the nitrogen NMR shift and that of the transition-metal nucleus. A range of square pyramidal complexes of cobalt(III) with a bent apical nitrosyl was therefore prepared and examined by ^{15}N and ^{59}Co NMR spectroscopy in a study of nephelauxetic and spectrochemical effects at the metal and nitrogen nuclei in the bent CoNO chromophore.[91] The basal ligands included dithiocarbamate, quadridentate Schiff base or porphine, and bischelating diamine or oximate, so as to give S_4, S_2N_2, N_4, OONN, or ONON coordination in the plane and a range of substituents in the chelate and phenylene rings; compounds are shown in Figure 3.

Energy-level diagrams have been calculated by the Wolfsberg−Helmholtz method for $[Co(NO)(NH_3)_5]^{2+}$ and related ions with different coordination geometries[99a] and by the extended Hückel method for nitrosyl bonded to five-coordinate iridum[99b] to show the orbital interactions as the nitrosyl bends. These results have been adapted in Figure 4 to show, schematically, the interrelation of the magnetically active excitation energies for ^{15}N and ^{59}Co in the bent nitrosyl complexes studied by ^{15}N and ^{59}Co NMR spectroscopy.[91] The d energy levels on the left of the diagram are appropriate to the umbrella shape of the basal ligands shown in Figure 3, in which the cobalt

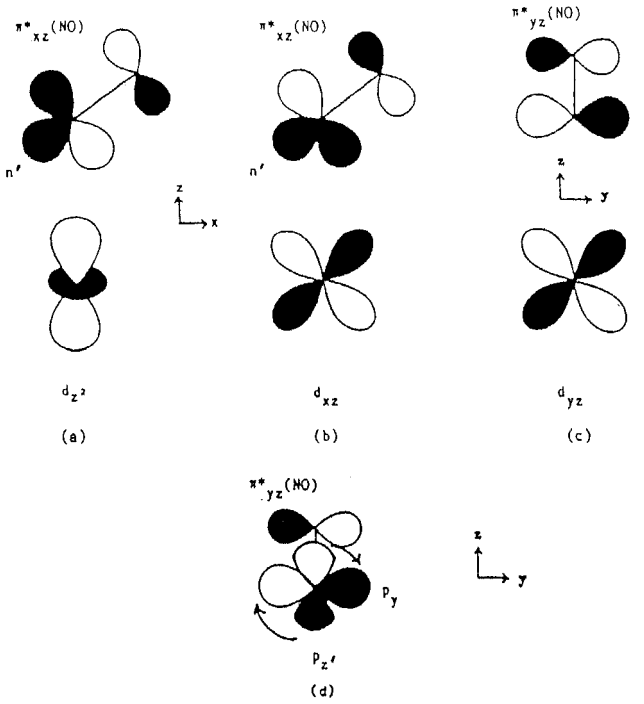

Figure 5. Diagrams showing interactions of n′(N) and π^*(NO) with d_{z^2} (a), d_{xz} (b), and d_{yz} (c) orbitals shown in Figure 4. (d) Diagram to illustrate a major paramagnetic circulation on nitrogen. (Reprinted with permission from ref 91. Copyright 1987 American Chemical Society.)

is 0.1−0.5 Å above the plane of the coligating atoms. The z^2 orbital is stabilized by s,p mixing, so as to point more in the direction of the vacant site trans to the nitrosyl, and is assumed to lie below the π^2-(NO) levels. The sequence and separation of the energy levels vary depending on the nature of the coligands, but the general conclusions are unchanged.

The d orbitals most strongly involved are the z^2 and *xz* orbitals in the MNO plane. Figure 5 shows their interaction with the *n′*(N) orbital (with σ-NO symmetry) and π^*_{xz}(NO) orbital of the ligand. Figure 5a shows that the destabilizing interaction of the occupied z^2 and *n′* orbitals is alleviated by bending of the MNO ligand by about 125° for the nitrosyls in question. This allows a bonding interaction of the z^2 and π^*_{xz}(NO) orbitals. Such bending reduces the back-bonding from *xz* to π^*_{xz}(NO) (Figure 5b), while the back-bonding in the *yz* plane is only slightly reduced (Figure 5c).

The lone pair on nitrogen, therefore, consists of nonbonding electron density in the MNO plane, which in the HOMO in Figure 4 is delocalized in the π^*_{xz}(NO) ligand orbital and in the *xz* and z^2 orbitals on the metal.

Figure 5d is a perspective view of the most important paramagnetic circulation determining the nitrogen shift, effectively *n*(N) → π^*(NO), using the a″ LUMO (in Figure 4) formed from the π^*_{yz} and *yz* orbitals (Figure 5c).

The atomic circulation on nitrogen shown in Figure 5d is of $p_{z^2} \rightarrow p_y$ type, with the p_{z^2} orbital at an angle of 35° to the *z* axis for a 125° MNO angle. In-plane and out-of-plane paramagnetic circulations of *n′*(σ-NO) → π^*(NO) type contribute also. The HOMO in Figure 4 is destabilized by the interaction with the z^2 orbital, the more so the greater the (σ + π) donation from the basal ligands. Weaker coligands, therefore, are expected to reduce the shielding of the nitrogen and cobalt, and coordination of a sixth ligand may have a similar effect. (If the z^2 orbital is sufficiently high-lying, then the mainly π^*(NO) orbitals are occupied in preference to ligand-field orbitals.)

Clearly, multiple factors are at work, but the extensive mixing of the π^*(NO) LUMOs with the x^2, *xz*, and *yz* orbitals acts to increase the shielding of both nitrogen and cobalt as back-bonding increases.

In practice,[91] the shielding of the nitrogen and the cobalt is found to (tend to) decrease with a decrease in the M(d) → π^*(NO) back-bonding, as indicated by the M−N and N═O bond lengths, the MNO angle, and the NO stretching frequency. The shieldings decrease from S → N → O coligators and decrease also with electron withdrawal by ring substituents, i.e., with a decrease in the ligand-field splitting and in the nephelauxetism of the coligands (and vice versa). Clearly, nephelauxetic and spectrochemical effects are interconnected for the cobalt and nitrogen nuclei. Strictly, nephelauxetism is defined for d electrons, but these systems clearly demonstrate analogous behavior to nephelauxetism for nonbonding p electrons such as the lone pair electrons on nitrogen.

The parallelisms of the cobalt and nitrogen shielding accord, therefore, with the orbital theory that was developed to explain the bending of the MNO ligand and the influences of the metal and coligands. The interdependence of the spectrochemical and nephelauxetic effects at cobalt and nitrogen arise from the degree of overlap and similar energies of the frontier orbitals for the two paramagnetic circulations, $n_N \rightarrow p^*$ around nitrogen and d−d around cobalt.

IV. Nitrogen Shielding Tensors in Metal Nitrosyls and Related Compounds[100]

Much more information, of course, is obtainable from shielding tensors than from chemical shifts; furthermore, measurements in the solid state are helpful for nitrosyls which are unstable or fluxional in solution. In five-coordinate {MNO}^{8} complexes, where 8 is the number of (d + n) electrons, the metal may have a trigonal-pyramidal coordination sphere (d^8) with the nitrosyl linear (NO^+) or else a square-pyramidal coordination sphere (d^6) with bent apical nitrosyl (NO^-) so may be fluxional in solution (similarly for diazenido ligands $N{=}NR^+$ and $N{=}NR^-$). The fluxions are: trigonal bipyramidal structure with linear nitrosyl ↔ square pyramidal structure with bent apical nitrosyl.

The first measurement of a nitrogen tensor in a metal complex was of $[RuCl(^{15}NO)_2(PPh_3)_2][BF_4]$, which has one linear and one bent nitrosyl in the solid state[101] and shows fast bent−linear fluxionality in solution.[46] The evidence of the nitrogen shifts in the solid state and in solution, showing a deshielding of ca. 35 ppm in the solid compared to the solution, accords with the evidence from the temperature-dependence of the equilibrium isotope effect (section I.F) for an additional contribution to the fluxional

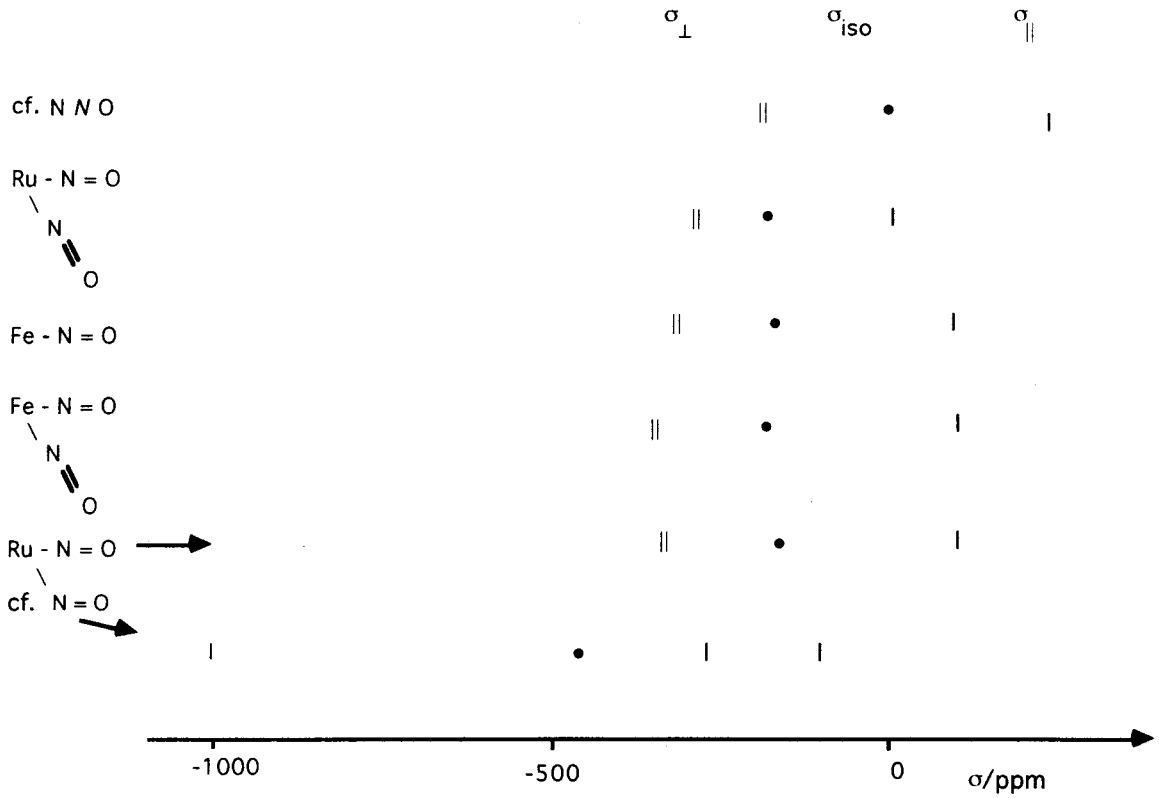

Figure 6. ^{15}N shielding tensors in the linear nitrosyl ligand.

process in solution, probably from a trigonal-bipyramidal structure with two linear nitrosyls.

Figures 6 and 7 and Tables 5 and 6 show the principal components of ^{15}N shielding tensors now known for linear and bent nitrosyls in complexes of iron and ruthenium measured in solid-state (CP-MAS) experiments compared with those of N_2O,[102] N_2O_2,[103] and N_2O_3[104] derived from spin-rotation measurements and of nitrobenzene[105] and nitrate ion from solid-state NMR.[106]

A. Nitrogen Shielding Tensors in Linear Nitrosyls

The measurements for the linear molecules HCN,[107] N_2,[108] and N_2O show that $\sigma_{||}$ for a C_8 axis is around 350 ppm, comparable to the diamagnetic shielding for free atomic nitrogen.[109] For the central nitrogen in N_2O, $\sigma_{||}$ is 364 ppm. Lower values in the near-linear ruthenium nitrosyls reflect deviations from linearity, with angles of 168−178°. As expected, the perpendicular shieldings are somewhat lower than for the two-coordinate nitrogen in NNO.

The $\sigma_{||}$ values in linear nitrosyls such as $[Fe(CO)_3(^{15}NO)]^-$ [110] are much more negative than for free NO^+: as expected, back-bonding to the nitrosyl ligand is likely to be greater than in the carbonyl ligand. The perpendicular components in the nitrosyls are more negative than in N*N*O and more negative in a bis- than in a mononitrosyl for the same metal; this is because bisnitrosyls are usually cis and the nitrosyls interact, bending slightly. Nitrogen shielding tensors have given the structure of $[Fe(NO)_2$(cystine)], which is amorphous and insoluble, so difficult to study by standard methods. The shielding tensors show that the nitrosyls are linear and probably cis.[111]

B. Comparisons of ^{15}N and ^{13}C Shielding Tensors in Linear Nitrosyls (MNO) and Metal Carbonyls (MCO)

Carbonyls are useful models for linear nitrosyls, since many ^{13}C tensors are known.[138] ^{13}C shielding ranges for transition-metal complexes M−CO are periodic, the perpendicular component $\sigma_\perp$ increasing across the row and down the group of the transition metal, and this is expected for linear nitrosyl ligands. For a given d-orbital configuration the ^{13}C shielding increases with increase in nuclear charge of the metal, as back-bonding decreases, as the d orbital energies fall below those of the carbon valence orbitals. Deshielding of ligating carbon or nitrogen correlates with lengthening and weakening of the bond to oxygen and shortening and strengthening of the bond to the metal. Deshielding is enhanced by *trans*-ligands such as polyhapto arenes, which are good charge donors, by a negative charge on the complex, and with an increase in the number of d electrons on a given metal, e.g., from $d^6 \rightarrow d^8 \rightarrow d^{10}$ complexes of cobalt.

The coordination shifts and NMR shielding tensors are consistent with deshielding of ligating nitrogen or carbon by an increase in π character in the bond to the metal. Deshielding with an increase in back-bonding has been correlated with stabilization of the π^*(CO) orbital[112] and of the $\sigma \rightarrow \pi^*$ state,[113] with the charge imbalance contribution to the paramagnetic term,[114] and with all three of these, in MO calculations;[115] it has also been correlated with a contribution from the direct field effect of d−d circulations on the metal, since π-donation to a carbonyl group correlates with increased carbon shielding in main-

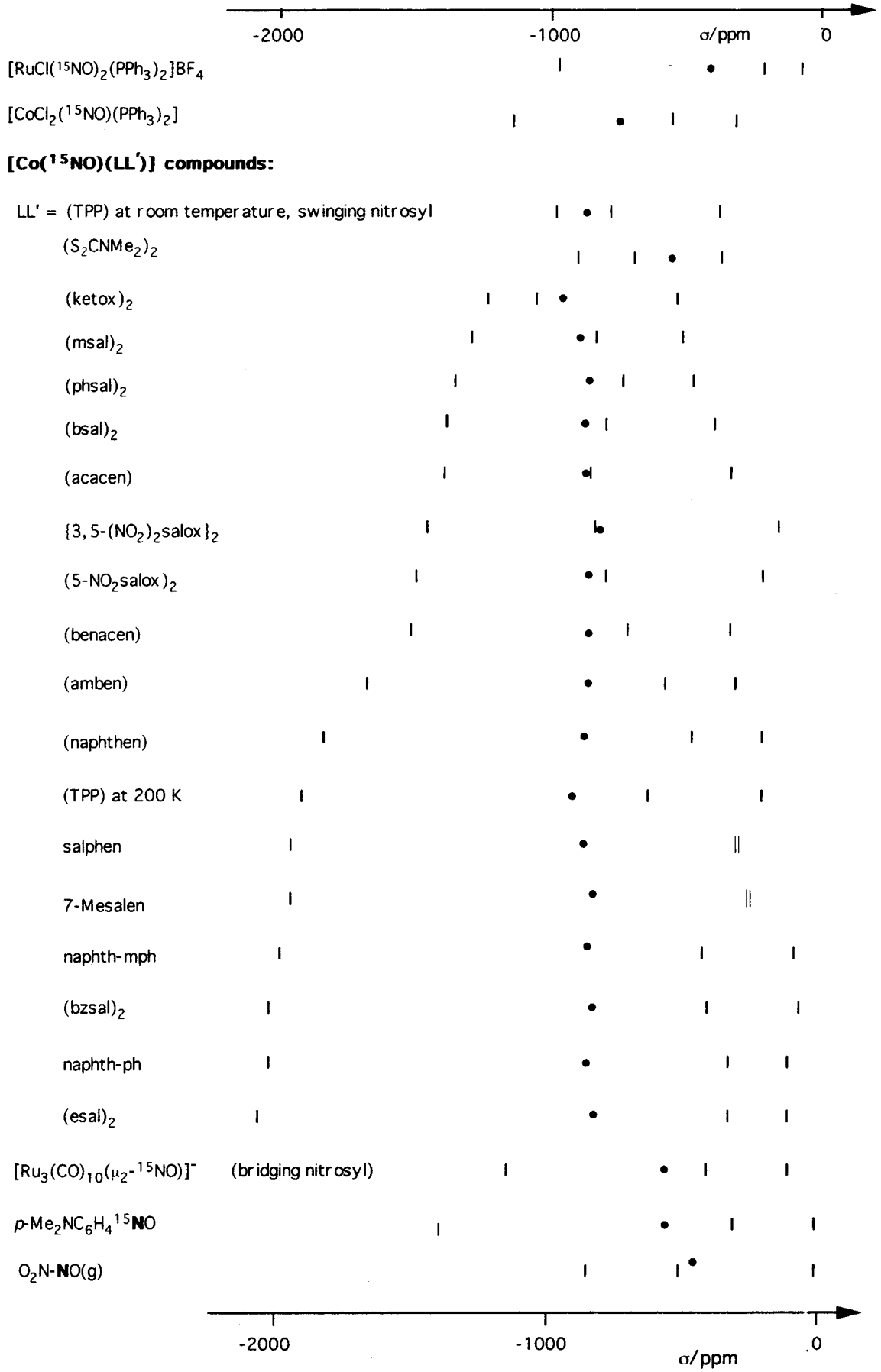

Figure 7. ^{15}N shielding tensors in bent or bridging nitrosyl ligands and in comparison compounds with bent or bridging nitrosyls.

Table 5. Principal Components of ^{15}N Shielding Tensors in Linear Nitrosyl Ligands in Metal Complexes and in Some Related Compounds

	δ_{iso}	σ_{iso}	$\sigma_{\perp}$	$\sigma_{\parallel}$	Ω	ref
*N*NO(g)	−240	105	−18	349	367	102
N*N*O(g)	−141	5	−174	364	538	102
$[Fe(CO)_3(^{15}NO)]^-$	18	−154	−295	127	422	108[a]
$[RuCl(^{15}NO)_2(PPh_3)_2][BF_4]$	26	−162	−309	133	442	101[b]
$[Ru(^{15}NO)_2(PPh_3)_2]$	37	−173	−284	48	332	*c*
	40	−176	−281	35	316	
$[Fe(^{15}NO)_2$(cystine)]	40	−176	−337	145	482	*c*

[a] Solution spectrum: Stevens, R. E.; Gladfelter, W. L. *Inorg. Chem*. **1983**, *22*, 2034. [PPN][$Fe(CO)_3(^{15}NO)$] structure: Pannell, K. H.; Chen, Y.-S.; Belknap, K.; Wu, C. C.; Bernal, I.; Creswick, M. W.; Huang, H. N. *Inorg. Chem*. **1983**, *22*, 48. [b] $[RuCl(^{15}NO)_2(PPh_3)_2][BF_4]$ structure: Pierpont, C. G.; Eisenberg, R. *Inorg. Chem*. **1972**, *11*, 1088. [c] Groombridge, C. J.; Larkworthy, L. F.; Mason, J. Manuscript in preparation.

group compounds.[116] The neighbor effects fall off as R^{-3} and are much less important for ligands other than H.

Extension of the π system from CO to O=C=O (and similarly for extension to O=C=C=C=O) stabilizes the σ(C) relative to the π^* orbitals, increasing the perpendicular shielding components, despite increases in the radial term due to the electronegative substituent. In the corresponding C/S molecules, $\sigma_{\perp}$ decreases with a decrease in orbital splittings.

Bridging carbonyl ligands, however, show small increases in the two 'perpendicular' components. Overall deshielding is due to a large decrease in the highest shielding component with loss of the high symmetry, with a greater decrease for doubly- than for triply bridging carbonyls, as expected.

C. Nitrogen Shielding Tensors in Bent Nitrosyls

Effects of bending of the nitrosyl ligand can be seen in the ruthenium complex with one linear nitrosyl and one bent, with ∠RuNO 138°: bending causes one of the perpendicular elements to plummet to a value of −994 ppm. This component σ_{33} is no doubt the one that mixes the nitrogen lone pair and π^*(NO) orbitals, the former being nonbonding and the latter very low-lying; the bending contributes also to σ_{33}. To study the factors that are involved, nitrogen shielding tensors were measured for a range of square pyramidal molecules with a bent apical nitrosyl. Molecular structures are given in Figure 3 and the tensor components in Table 6. Figure 7 shows graphically the very interesting variations in nitrogen shielding tensor for these molecules and some others with bent nitrosyls, including *p*-nitroso-*N*,*N*-dimethylaniline.[117]

In some of the square-pyramidal complexes the planarity of the basal ligand is maintained by chemical bonding or strong hydrogen bonding. In the others, the nitrogen tensor components are a useful proof of the pyramidal structure, since not all of the bis-chelate compounds are constrained to coplanarity: in the [Co(NO)(Rsal)$_2$] series the parent com-

Table 6. Principal Components of ^{15}N Shielding Tensors in Bent or Bridging Nitrosyl Ligands and in Some Comparison Compounds with Bent or Bridging Nitrosyls[100]

										ref	
compound	∠MNO/°	δ_{iso}	σ_{iso}	σ_{11}	σ_{22}	σ_{33}	Ω	κ	δ_{soln}	NMR	structure[a]
$[RuCl(^{15}NO)_2(PPh_3)_2]BF_4$	136.0	303	−439	−994	−229	−94	900	0.700	flux.	*c*	
$[CoCl_2(^{15}NO)(PPh_3)_2]$		531	−667	−1149	−550	−301	848	0.414	flux.	*d*	
$[Co(^{15}NO)(LL')_2]$:											
LL′ = $(S_2CNMe_2)_2$	135.1	499	−535	−877	−672	−357	520	−0.790	501	*d*	*l*
{3,5-$NO_2)_2$salox$_2$		679	−815	−1458	−839	−148	1310	−0.055	n.o.	*d*	
(5-NO_2salox)		682	−818	−1479	−786	−189	1290	0.074	833.1	*d*	
(salen)	127	698	−835	−2050	−302	−151	1884	−0.85	725.4	*e*	
(naphthen)		709	−875	−1819	−478	−226	1593	−0.898	n.o.	*d*	
(naph-ph)		711	−847	−2069	−357	−113	1956	0.752	n.o.	*d*	
(7-Mesalen)		714	−850	−1968	−291	−291	1677	1.000	710.0	*d*	
(salphen)		717	−853	−1963	−296	−296	1667	1.000	769.7	*d*	
$(phsal)_2$		720	−856	−1348	−740	−480	868	0.401	n.o.	*f*	
(benacen)	123	721	−857	−1536	−707	−327	1209	0.372	723.0	*d*	*m*
(amben)		721	−857	−1681	−576	−315	1366	0.617	734.3	*d*	
(naphth-mph)		721	−857	−1894	−496	−183	1711	0.633	n.o.	*d*	
$(bzsal)_2$		722	−858	−2058	−427	−89	1969	0.657	530.2	*f*	
(acacen)	122	723	−859	−1402	−850	−326	1076	0.025	714.3	*d*	*m*
$(bsal)_2$		728	−864	−1398	−805	−390	1008	0.176	740.5	*f*	
$(msal)_2$		735	−871	−1273	−826	−510	763	0.177	n.o.	*f*	
$(esal)_2$	129	742	−878	−2095	−376	−162	1933	0.779	739.7	*f*	
(TPP) 298 K	127	765	−901	−1062	−820	−820	242	1.0	770.7	*g*	*n*
(TPP) 220 K		758	−893	−1072	−804	−804	268	1.0		*g*	
(TPP) 200 K		757	−893	−1853	−626	−198	1655	0.484		*g*	
$(ketox)_2$	126.3	781	−917	−1260	−1007	−484	776	−0.348	740.3	*f*	*o*
cf. $[Ru_3(CO)_{10}(\mu$-$^{15}NO)]^-$[b]		424	−560	−1160	−408	−112	1048	0.435	434	*h*	
$Ph^{15}N(O)^{15}N(O)Ph$			−66	−220	−43	65	285	0.242		*i*	
O_2N-*N*O(g)		292	−428	−860	−435	10	870	−0.024		*j*	
p-$Me_2NC_6H_4{}^{15}NO$		445	−581	−1457	−309	22	1479	0.55		*i*	
O=N−N=O(g)		1835	−1971	−5278	−592	−44	5322	0.78		*k*	

[a] If reported separately from the NMR studies. [b] Bridging NO. [c] Reference 101. [d] Groombridge, C. J.; Larkworthy, L. F.; Mason, J. Unpublished results. [e] Barrie, P.; Larkworthy, L. F.; Mason, J. Unpublished results. [f] Reference 86. [g] Reference 96. [h] Reference 108. [i] Reference 115. [i] Calculated from spin-rotation constants given by Kukolich, ref 14. [j] Malli, G.; Froese, C. *Int. J. Quantum Chem*. **1967**, *1s*, 95. [k] Calculated from spin-rotation constants given by Kukolich, ref 119, see text. [l] Enemark, J. H.; Feltham, R. D. *J. Chem. Soc., Dalton Trans*. **1972,** 718. [m] Wiest, R.; Weiss, R. *J. Organomet. Chem*. **1971**, *30*, C33. Wiest, R.; Weiss, R. *Rev. Chim. Miner*. **1972**, *9*, 655. [n] Reference 95. [o] Larkworthy, L. F.; Povey, D. C. *J. Cryst. Spectrosc. Res*. **1983**, *13*, 413.

plexes $[Co(Rsal)_2]$ are tetrahedrally coordinate. Although $[CoCl_2(^{15}NO)(PPh_3)_2]$ shows bent−linear fluxionality in solution, the tensor properties show that the nitrosyl is bent in the solid.

All three tensor components for bent nitrosyls show significant deshielding compared with those in linear nitrosyls: the σ_{11} values for bent nitrosyls are strongly negative and variable. The bridging nitrosyl in $[Ru_3(CO)_{16}(\mu_2\text{-NO})]^-$ shows relatively high σ_{11} shielding and σ_{33} also is rather high, since the nitrogen is three-coordinate (Ru_2NO) and the lowest-energy excitations are now $\sigma \leftrightarrow \pi$. S_4-ligation of cobalt increases the nitrogen shielding, as expected, because of higher excitation energies for ligating atoms from the third than from the second row of the Periodic Table.

The apical nitrosyl shielding tensors in Figure 7 show a remarkable variation in the span (Ω) and skew (κ), while the isotropic shift δ remains at 680−780 ppm. The span and skew are defined as

$$\Omega = \sigma_{33} - \sigma_{11} = \delta_{11} - \delta_{33}\ \kappa = 3(\sigma_{iso} - \sigma_{22})/(\sigma_{33} - \sigma_{11}) \quad (8)$$

All components reflect significant mixing of the nitrogen and the cobalt paramagnetic circulations (more precisely, the out-of-plane components of the ligand-field circulations deshielding cobalt), as discussed in section III.C.[91]

The variations in tensor components may include effects of different positioning of the nitrosyl ligand relative to coligands in the plane (over an electron acceptor, for example) because of large effects of relatively small changes in small excitation energies. Nitrosyl oxygen lies above a gap between two chelate ligands in $[Co(NO)(ketox)_2]$ and $[Co(NO)(esal)_2]$, over the ethylene bridge in [Co(NO)(7-Mesalen)] and [Co(NO)(salen)], over a linear nitrosyl in $[RuCl(^{15}NO)_2(PPh_3)_2]^+$, over sulfur in $[Co(NO)(S_2CNMe_2)_2]$, over oxygen in [Co(NO)(acacen)], and over nitrogen in [Co(NO)(benacen)]. The ligand field and the shieldings are of course sensitive to the internal MNO geometry, to the location of cobalt, which is usually above the plane, to the ligation, and to the bite of the chelate ligands.

An additional factor is the possibility of swinging or spinning of the nitrosyl group. There is rotational disorder in some of the crystal structures, so the torsional barrier must be small. Torsional variation and sensitivity of the projecting nitrosyl to intermolecular forces could account for compensatory effects in the tensor components: σ_{22} and σ_{33} decreasing as σ_{11} increases, decreasing the span Ω while maintaining the isotropic shift. This hypothesis was tested by measurements of the nitrogen shielding tensor in $[Co(^{15}NO)TPP]$ at lower temperatures to reduce any motion of the nitrosyl group, as shown in Figure 8.

The 'contracted' nitrogen tensor observed for $[Co(^{15}NO)(TPP)]$ at ambient temperatures was found, indeed, to be due to swinging or spinning of the nitrosyl ligand in the solid state.[96] Although the isotropic shift is that of a bent nitrosyl, the shielding tensor, from room temperature down to 220 K, shows axial symmetry ($\kappa = 1$) and a small span, 242 ppm.

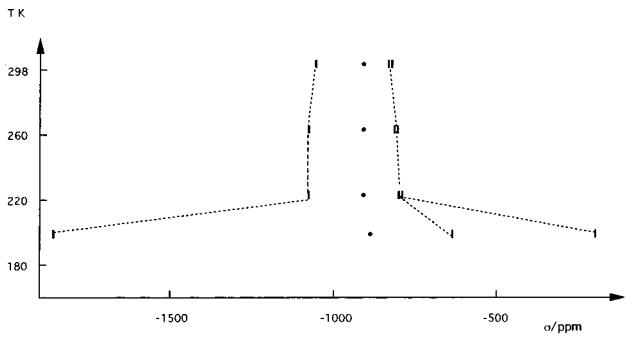

Figure 8. ^{15}N shielding tensors for $[Co(^{15}NO)TPP]$; changes on cooling to 200 K.

However, when the sample was cooled to 200 K, the full span of 1655 ppm appeared and nonaxial symmetry was evident ($\kappa = 0.484$), with little change in isotropic shift, as shown in Figure 8. No intermediate rate behavior could be observed.

Differential scanning calorimetry showed a phase transition in the solid at 206.7 K, with $\Delta H = 649$ J mol^{-1}. At this temperature, presumably, the lattice relaxes to allow the nitrosyl to revolve about the C_4 axis. A CoNO angle of 127° calculated from the tensor measurements agrees with the value ≤128.5° estimated from Scheidt and Hoard's X-ray diffraction study at ambient temperatures.[118] The X-ray work showed a 2-fold disorder of the cobalt relative to the TPP plane and 4-fold disorder of the nitrosyl (in a given orientation), which they depicted in a many-headed 'hydra' diagram (Figure 7). The oxygen lies in the gap between two porphin nitrogens, pointing toward a pendant phenyl group. This picture, therefore, is that of a spinning, or more likely swinging, nitrosyl.

Figure 7 shows graphically that several of the nitrosyls, measured at room temperature, have motional freedom resembling that of the [Co(NO)(TPP)] nitrosyl. It is likely, therefore, that anisotropies recorded for bent nitrosyls may have been reduced and asymmetries η increased by small-angle oscillations of the nitrosyl ligand. Figure 7 suggests also that certain substituents in the basal ligands, as in the $[Co(NO(Rsal)_2)$ compounds, may be obstructing torsional motion of the bent nitrosyl: particularly broad spans are observed with ethyl and benzyl R substituents.

Table 6 and Figure 7 include for comparison bent nitrosyl tensors measured for nitrogen oxides and organic nitroso compounds. For N_2O_3 (O_2N-NO), pulsed beam microwave studies showed some spin-rotation hyperfine structure, giving one spin-rotation constant for each nitrogen.[119] Approximate values of the principal components were estimated[120] from the solution shifts[121] using perpendicular shielding components comparable to those in related molecules.

For the interesting near-rectangular nitric oxide dimer O=N−N=O, which is the main component of liquid or solid NO, tensor elements were estimated from the spin-rotation constants determined by molecular beam electric resonance spectroscopy[122] with uncertainties of about 200 ppm for σ_{33} and σ_{11} and 40 ppm for σ_{22}. N_2O_2 has a remarkably long N−N bond (2.33 Å), and the perpendicular tensor element

−5280 ppm corresponds to an enormous isotropic shift, $\delta = 5140$. Other properties also show the relevant excited state(s) to be extremely low; thus, the $n_N-\pi^*$ absorption is in the near infrared, so that N_2O_2 is colorless, and shows temperature-independent paramagnetism.

V. Theoretical Studies of Nitrogen Shielding Tensors in Metal Nitrosyls and Related Compounds (E. A. Moore)

In nonrelativistic calculations nuclear magnetic shielding can be divided into two terms. The diamagnetic term, arising from circulations of electrons in ground-state orbitals (acting to oppose the applied field) is relatively easy to calculate. The paramagnetic contribution, reinforcing the applied field, which dominates the shielding of elements other than hydrogen in their compounds, is harder to calculate since it involves circulations between occupied ground-state orbitals and appropriate excited-state orbitals.

In terms of the density matrix, the *ji*th component of the paramagnetic component σ^p_{ji} of the shielding tensor is given by

$$\sigma^p_{ji} = \langle h^{m_{nj}} \mathbf{P}^{B_i} \rangle \quad (9)$$

where $\mathbf{P}^{B_i}$ is the derivative of the density matrix with respect to the external magnetic field and $h^{m_{nj}}$ is the matrix element of the derivative of the one-electron Hamiltonian with respect to the field due to the magnetic nucleus. Until recently, most calculations used a variant of the coupled Hartree−Fock method in which coupled perturbed equations are solved to give the derivative of the density matrix, with respect to the external field, which can then be combined with the matrix element of the perturbation due to the magnetic nucleus to give the shielding as in eq 9.

The external magnetic field has an arbitrary gauge origin. The calculated shielding is independent of the origin chosen if a complete basis set is used, but early calculations with small basis sets showed a marked dependence on the choice of origin. Several methods have been developed to overcome this problem. The best known is the GIAO method[123] (gauge-including atomic orbitals), in which the atomic orbitals are modified by an exponential term involving the gauge in order to obtain the derivative of the density matrix with respect to the external field. The IGLO method (individual gauge localized orbitals)[124] is similar except that modified localized molecular orbitals are used in place of atomic orbitals. The LORG (localized orbital/local origin) method[125] places the gauge origin at the centroid of charge of each localized orbital, and the newer CGST (continuous set of gauge transformations) method[126] uses a separate gauge origin for each point in space.

Much progress has been made in calculating shielding tensors using these methods, but tensors for compounds containing lone pairs, as in bent nitrosyls, have proved difficult. One source of difficulty is the presence of low-lying excited states, as in the $n_N-\pi^*$ excitation, for which electron correlation becomes important. The earliest method used for this was to include a second-order correction to the wave function, the Møller−Plesset (MP2) term.

The multiconfigurational approach is more accurate but much more expensive of computer resource. Some success has been achieved more recently with density functional methods (DFT), which are less accurate then the multiconfigurational approach but use considerably less computer resource.

Schindler and Kutzelnigg[127] applied the IGLO method to a number of small molecules, including linear N_2O and bent NOF, with an ONF bond angle of 110°. The main contributions to the paramagnetic shielding came from the NN and NO σ bonds. The IGLO method reproduced the isotropic shielding of N**N**O fairly well but considerably overestimated the paramagnetic shielding of the perpendicular component.

Overestimation of a large paramagnetic component is a feature of Hartree−Fock studies of NO-containing molecules. For nitrogen in NOF, the main contributors to the paramagnetic term were from the nitrogen lone pair and the N═O bond, particularly for one of the in-plane components, σ_{yy}. This study used triple-ζ basis sets with polarization functions. The authors believed that they were close to the Hartree−Fock limit and that further improvement would require the inclusion of some allowance for electron correlation. This conclusion was borne out by a later study of N_2O using GIAO, which improved agreement with experiment[128] by including the second-order Møller−Plesset (MP2) correction for electron correlation, with some improvement also by the use of density functional methods.

Since the dinitrogen oxides N_2O_2, N_2O_3, and N_2O_4 all have long N−N bonds, their low-lying orbitals make a large paramagnetic contribution to the shielding tensors, which are particularly difficult to calculate. IGLO calculations[129] for N_2O_4 were found to overestimate the paramagnetic contribution, but the use of multiconfiguration wave functions (MC−IGLO) produced a value for the isotropic shielding (−125 ppm) very close to the experimental value (−123 ppm).

For N_2O_3, with the ON−NO_2 structure, close agreement was obtained with the experimental shielding tensor for the NO_2 nitrogen by the use of MC−IGLO[127] and DFT[130] methods. As expected, Hartree−Fock IGLO[127] calculations, LORG,[130] and GIAO[130] gave isotropic shieldings that were more negative than the experimental values. For the NO nitrogen Hartree−Fock methods, perhaps surprisingly, reproduced the isotropic shielding well: IGLO gave −407 ppm, LORG −391 ppm, and GIAO −396 ppm compared with −428 ppm by experiment. The principal components of the shielding tensor were not well reproduced. Interestingly, in this case the use of MP2 or DFT methods resulted in an *increase* in the paramagnetic term, by 200−450 ppm, in contrast to most other −NO results. MC−IGLO calculations also increased the paramagnetic term somewhat, by 63 ppm. Agreement with experimental values of the principal components was only fair, even for multiconfiguration calculations.

There was remarkably good agreement between the calculated and experimental ^{15}N shielding tensor for the doubly bent N_2O_2 molecule using MC−IGLO.[127] Because of the exceptionally long, weak NN bond the nitrogen has an unusually large paramagnetic shielding, larger for MC−IGLO than for IGLO calculations. The increase is most striking for the *zz* component, perpendicular to the NN bond in the molecular plane. IGLO gives this component as −2215 ppm and MC−IGLO −4414 ppm compared with an experimental value around −5278 ppm.

In an study of nitrite and nitrate ions,[131] good agreement of experimental and calculated shielding tensors was found for nitrate ion by the LORG method with a medium-sized basis set and including the second-order Møller−Plesset correction for correlation. The same method applied to the (bent) nitrite anions with cations around it gave reasonable agreement for the isotropic shielding and two of the principal components. The calculated out-of-plane component of the tensor was considerably larger, however, than the experimental value. An IGLO calculation[127] for the free nitrite ion gave a much larger negative value for the shielding than experiment, but the use of multiconfigurational (MC) IGLO produced a value very close to experiment.

Wasylishen et al.[132] calculated ^{15}N chemical shifts for model organic nitroso compounds $H_2C{=}CH(NO)$ and $O^-HN^+{=}N^+HO^-$ using LORG. The results were useful in indicating the orientation of the shielding tensor for the compounds they measured experimentally, the nitrosobenzene dimer and 4-nitroso-*N*,*N*-dimethylaniline. Even allowing for the change in electron distribution from H to a conjugated benzene system, the calculations were thought to overestimate the paramagnetic term, especially for the low-shielding component: the authors suggest that the inclusion of electron correlation in the calculations might improve the agreement.

Given the difficulty of accurate calculations of nitrogen shielding tensors for small molecules, calculating tensors for NO attached to a metal might be considered impractical. Several recent studies have shown, however, that DFT methods can usefully be applied to ^{15}N shielding in metal nitrosyl complexes. All the complexes studied were square pyramidal with bent apical MNO, resembling the geometry of NO bound to heme. A DFT-IGLO study[133] of a model based on [Co(NO)(TPP)] showed the extreme sensitivity of the nitrogen shielding to changes in CoNO geometry. The isotropic shielding was shown to decrease rapidly with an increase in the Co−N distance and even more rapidly with an increase in the N−O distance. This sensitivity arises mostly from the changes in σ_{11} with the 1 axis parallel to the N−O bond.

The variation in shielding with CoNO bond angle was calculated with fixed Co−N and N−O distances. The isotropic shielding increased with an increase in the CoN=O angle from 120° to 170°, although σ_{11} first decreases and then increases. In a study of iron and cobalt metalloporphyrin and metalloprotein analogues[134] DFT-GIAO calculations were carried out on model Co−N=O and Fe−N=O complexes. The calculated isotropic shifts obtained compared very well with the experimental values for the parent compounds. There was also good agreement with the tensor elements for the iron complexes, less good for the cobalt complexes.

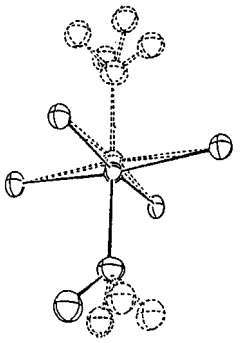

Figure 9. Statistical disorder in [Co(NO)TPP]: a single orientation of the Co(NO)(N_4) group is shown in solid lines. (Reprinted with permission from ref 95. Copyright 1993 American Chemical Society.)

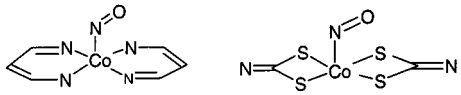

Figure 10. Model compounds for theoretical calculations.

DFT-GIAO calculations[135] on model square-pyramidal complexes of cobalt (porphinato, oximato, and dithiocarbamato) with bent apical nitrosyl, as shown in Figure 10, confirmed the variation in the nitrogen shielding with Co−N and N=O distance, with the same pattern of variation for the dithiocarbamato as for the model porphin complexes. Figure 11 shows the variation of nitrogen shielding with NO distance for different model complexes, with the same pattern for all the basal ligating atoms studied.

The model porphin structure $Co(C_3N_2H_5)_2NO$ is small enough for shielding calculations to be performed using the available computer resource and is found to represent the main features of metal porphins.

Figure 12 shows the variation of the shielding with Co−N distance. Note that the slope is steeper in Figure 11 than Figure 12.

For all the models in this study, the shielding first decreases then increases with increasing CoNO angle, as in Figure 13, following the variation of σ_{11}.

The studies confirmed that the variation in shielding with CoN=O distance is as expected if the excitation energy is the dominant term. Large negative values of σ_{11} and hence σ_{iso} arise primarily from the paramagnetic contribution of the *n*(N) orbital, because of the low energy of the $n(N)\rightarrow\pi^*(NO)$ circulation around the NO bond in the magnetic field. As the NO bond lengthens, the π bonding weakens, lowering the π^*(NO) orbital. The shielding is less sensitive to changes in Co−N distance, but again the variation is primarily determined by the change in $n-\pi^*$ energy. This dependence is shown in Figure 14, a plot for dithiocarbamato cobalt nitrosyls showing the decrease in isotropic shielding with increase in $\Delta E^{-1}[n(N)\rightarrow\pi^*(NO)]$ with change in the N=O and Co−N distances.

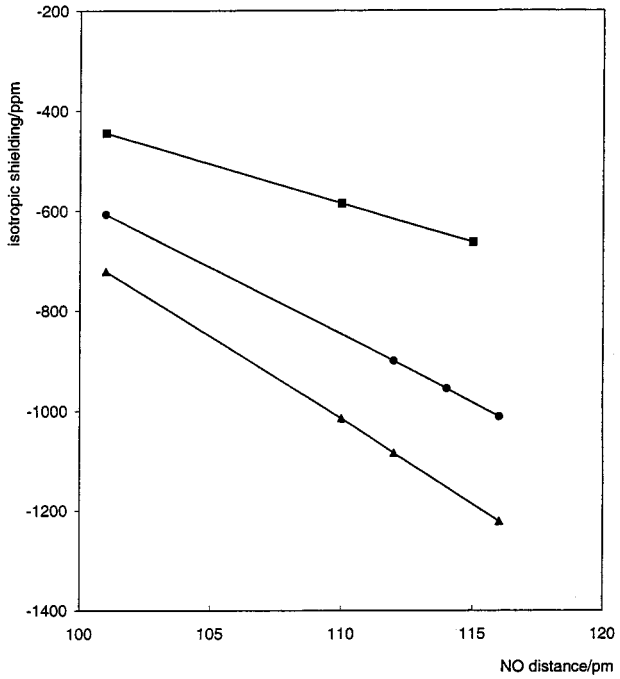

Figure 11. Calculated nitrogen shieldings with variation of the N═O distance for model complexes of cobalt: (■) porphins $Co(C_3N_2H_5)_2NO$ with r(CoN) = 183 pm and CoNO angle 127° (ref 133); (●) porphins $Co(C_3N_2H_5)_2NO$ with r(CoN) = 173.8 pm and CoNO angle 120° (ref 135); (▲) dithiocarbamates $Co(S_2CNH)_2NO$ with r(CoN) = 183 pm and CoNO angle 120° (ref 135).

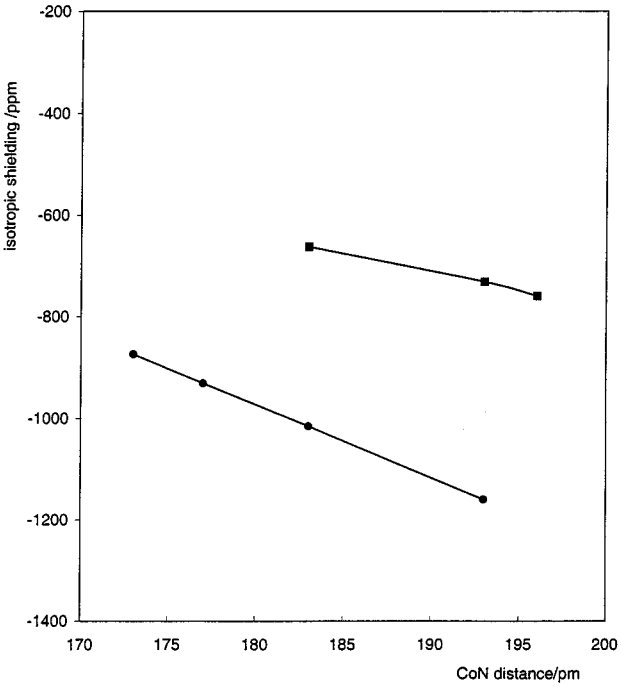

Figure 12. Calculated nitrogen shieldings with variation of the Co−N distance for model complexes of cobalt: (■) porphins $Co(C_3N_2H_5)_2NO$ with r(N═O) = 115pm and CoNO angle 127° (ref 133). (●) cobalt dithiocarbamato model complexes $Co(S_2CNH)_2NO$ with r(N═O) = 110pm and CoN═O angle 120° (ref 135).

The calculated $n-\pi^*$ energy gap increases with increasing angle as the $d_{z^2}-\pi^*$(NO) overlap decreases, but the variation in isotropic shielding with CoNO angle is proportional to the reciprocal of this energy difference only for angles below 140°. As the angle approaches 180°, the nature of the orbitals change, such that the n−π^* circulation is no longer responsible for the paramagnetic circulation, and the shielding actually increases with a decrease in $\Delta E^{-1}[n(\mathrm{N})\rightarrow\pi^*(\mathrm{NO})]$.

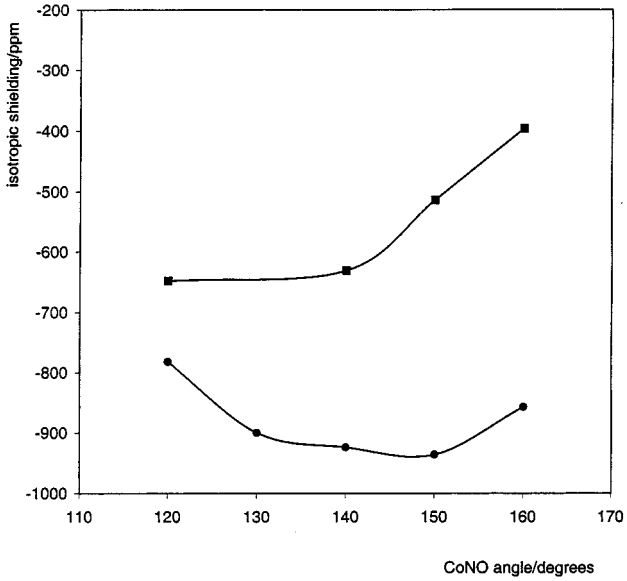

Figure 13. Calculated nitrogen shieldings with variation of the CoNO angle for model complexes of cobalt: (■) porphins $[Co(C_3N_2H_5)_2NO]$ with r(N═O) = 110 pm and r(Co−N) =193 pm (ref 133); (●) dithiocarbamates $[Co(S_2CNH)_2NO]$ with r(N═O) = 110 pm and r(Co−N) = 172.8 pm (ref 135).

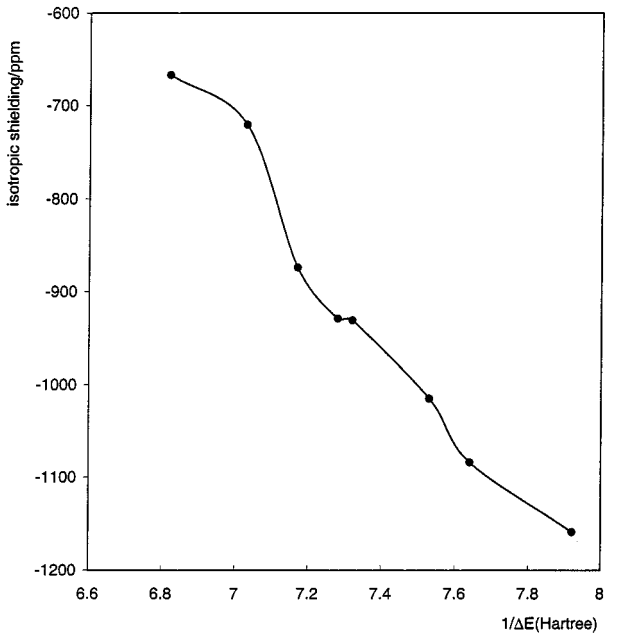

Figure 14. Calculated variation in nitrogen shielding with $\Delta E^{-1}(n\text{-}\pi^*)$ for model dithiocarbamato complexes $[Co(S_2CNH)_2NO]$ with CoNO angle 120° (ref 135).

VI. Patterns of Spin–Spin Couplings in Nitrosyls and Related Compounds[136]

Couplings producing a 1:1 doublet in ^{15}N resonance produce a 1:1:1 triplet with ^{14}N, for which $I = 1$. $J(^{14}NX)$ values are 30% smaller than $J(^{15}NX)$ values and opposite in sign, following the values of the

magnetogyric ratio γ where n is the number of bonds

$$^{n}J(^{15}\mathrm{NX}) = 1.403\ ^{n}J(^{14}\mathrm{NX}) = {}^{n}K(\mathrm{NX})h\gamma_{\mathrm{N}}\gamma_{\mathrm{X}}/4\pi^{2} \quad (10)$$

in the coupling pathway and J is in Hertz. Signs are usefully discussed in terms of the reduced coupling constant K/N A^{-2} m^{-3} since $\gamma(^{15}\mathrm{N})$ is negative.

Couplings to nitrogen are relatively small because of small γ values (Table 1). Spin−spin coupling measurements in nitrosyls are limited by the oxygen nuclear quadrupole and usually involve ^{15}N. Couplings to ^{14}N are observable when the local electronic symmetry is high and correlation times are short, as in supercritical fluids; couplings $^{1}J(^{14}\mathrm{N}^{14}\mathrm{N}) = 4.5$ Hz and $^{1}J(^{14}\mathrm{N}^{17}\mathrm{O}) = 37$ Hz were observed in neat supercritical $^{14}N_2$17O; $^{2}J(^{14}\mathrm{N}^{17}\mathrm{O}) < 5$ Hz in subcritical $^{14}\mathrm{N}^{17}\mathrm{O}$ at 28 °C. The sample exploded above the critical point, 40 °C.[137]

Fermi contact interaction of s electrons with the nucleus is usually the most important contribution to the coupling. Nitrogen couplings, therefore, are stereochemically sensitive to the angle at nitrogen, to the presence and orientation of a lone pair with s character on the nitrogen, and to the s,p character of the bonding as well as to medium effects. Couplings increase in magnitude regardless of sign with an increase in electronegativity of the substituents on a coupled nucleus. Lone pair contributions to the coupling may be large because of the small energy denominator for nonbonding electrons. Relationships of ^{1}J values to %s character in the bonds allow coupling constants to be estimated to optimize experimental parameters.

$^{1}J(^{15}\mathrm{NH})$ values are negative, the more so with increasing s-character in the N−H bonding orbital, from NH_4^+ or amines (sp^3) to pyridinium ion pyH^+ (sp^2) and to nitrilium ion $RC{\equiv}NH^+$ (sp). They diminish with an increase in (s-type) lone pair electron density on nitrogen and thus are very small for bent nitrogen in diazenides M−N=NH, increasing in magnitude on coordination, delocalization, protonation. or hydrogen bonding of the nitrogen.

$^{1}J(^{13}\mathrm{C}^{15}\mathrm{N})$ values become more negative from azomethines $R_2{}^{13}C{=}{}^{15}NR$, with a lone pair on nitrogen, to amines, and to ynamines.

The largest magnitudes of couplings are observed in linear systems. In ligands such as nitrosyl which may be bent or linear in their attachment to a metal, M−N_α coupling constants are reduced on bending and protonation of the bent nitrogen greatly increases $^{1}J(\mathrm{M}^{15}\mathrm{N})$.[125] Couplings are enhanced also by flattening of a pyramidal group, delocalizing s-type lone pair electron density.

Contact, orbital, and spin−dipolar contributions to the coupling have been discussed.[138−141] $^{1}J(^{15}\mathrm{N}^{15}\mathrm{N})$ values are small and negative when they involve terminal nitrogen, as in N_2O, very small in arene−diazonium compounds $ArNN^+$.[142] Couplings increase in absolute magnitude with an increase in s character in the bonding orbitals between the coupled nuclei and with more electronegative substituents.

^{1}J(CN) is commonly negative, as are $^{1}J(^{15}\mathrm{NY})$ values in general. $|^{1}J(^{15}\mathrm{CN})|$ is smaller if nitrogen carries a lone pair (the more so as its s character increases, as from amines to pyridine, sp^3 to sp^2) and may become positive, as in pyridine,[143a] changing sign on protonation of the nitrogen, becoming more negative in the *N*-oxide. Since pyramidal nitrogen in oximes $R_2C{=}NOH$ is flatter in the *Z* form than in the *E* form, to reduce *cis*-repulsions, $^{1}J(^{13}\mathrm{C}^{15}\mathrm{N})$ is more negative in the *Z* form.

Noncontact contributions also increase in magnitude when there are electronegative substituents on the coupled nuclei, because of a dependence on the radial term $\langle r^{-3}\rangle_{2p}$. Contact and noncontact contributions are all large in the benzonitrile *N*-oxide 2,4,6-$C_6Me_3H_2CNO$, giving an unusual value of $^{1}J(^{13}\mathrm{C}^{15}\mathrm{N}) = -77$ Hz.[144a]

Nitrogen spin−spin couplings to other nuclei are normally dominated by the contact interaction and thus are sensitive to s character in the relevant bonding orbitals and to the presence of lone pair electrons.

Periodic trends can be rationalized in terms of stabilization of bonding σ MOs and destabilization of nonbonding (lone pair) MOs with an increase in atomic number down the group or across the row of the Periodic Table. ^{1}K(CN) and ^{1}K(SiN) values are normally positive, but ^{1}K(SnN) values may be of either sign and ^{1}K(PbN) values are negative. Couplings to transition metals are normally positive. $^{1}J(^{59}\mathrm{Co}^{15}\mathrm{N})$ couplings of ±36−74 Hz are reported for cobaloximes containing ^{15}N-labeled pyridine or aniline ligands in the solid state, −36 and −75 Hz in cobaloximes, cf. 7.2 and 17.8 Hz for $^{1}J(^{103}\mathrm{Rh}^{15}\mathrm{N})$ in rhodoximes.[144b]

Ligating nitrogen is relatively low (above halides or alkoxy ligands) in empirical series of *trans*-influence, the tendency of a ligand forming a strong bond to the metal to weaken the *trans*-bond, reducing the magnitude of the trans coupling constants involving the trans bond.

VII. Dynamic Processes Observed in Nitrogen Resonance

Dynamic processes with a range of time scales have been monitored by relaxation and NOE measurements in nitrogen resonance.[1,2,4] Hindered motions about N−X bonds have been studied by line shape analysis, 2D spectroscopy, multicoalescence experiments, saturation transfer, equilibration methods, or relaxation time measurements. Studies of isomerization processes involving N−X bonds have been reviewed.[145]

^{14,15}N spectroscopy has demonstrated kicking motions, as in the bent−linear fluxionality in solution of the imido ligand M=NH in concert with a second imido or an alkoxy ligand.[139] A corresponding fluxionality of nitrosyls in solution was observed for the five-coordinate complex $[RuCl(^{15}NO)_2(PPh_3)_2]^+$. The averaged shift, the temperature dependence, and the equilibrium isotope effect with semienrichment are in accordance with a dynamic equilibrium between a trigonal-bipyramidal form with two linear nitrosyls and a square-pyramidal form with one bent and one linear nitrosyl. Polymorphs, which include intermediate forms, can be obtained in the solid state. As described in section IV, swinging and spinning of the

bent apical nitrosyl in solid [Co(^{15}N)(TPP)] at room temperature was confirmed through changes in the nitrogen shielding tensor as the temperature was lowered. The nitrogen shielding tensors determined for other square-pyramidal nitrosyls suggest similar motions, as discussed in section IV.

CIDNP, chemically induced dynamic nuclear polarization, enhancing absorption or emission, has been used in ^{15}N NMR studies of migrations of nitro groups,[146] azo-coupling,[147] loss of N_2 from arenediazonium salts,[148] and stable nitroxide radicals.[149]

VIII. References

(1) Mason, J. In *Encyclopedia of Nuclear Magnetic Resonance*; Wiley: New York, 1996; Vol. 5, p 3222.
(2) Mason, J. Nitrogen. In *Multinuclear NMR*; Mason, J., Ed.; Plenum: New York, 1987: Chapter 12, p 335. Mason, J. *Chem. Rev.* **1981**, *81*, 205. Mason, J. *Chem. Br.* **1983**, 654.
(3) Kini, A. D.; Washington, J.; Kubiak, C. P.; Morimoto, B. H. *Inorg. Chem.* **1996**, *35*, 6904 and references therein.
(4) Hoshino, M.; Laverman, L.; Ford, P. C. *Coord. Chem. Rev.* **1999**, *187*, 75 and references therein. For spectroelectrochemistry of Co(NO) porphyrins, see: Richter-Addo, G. B.; Hodge, S. J.; Yi, G.-B.; Khan, M. A.; Ma, T.; Van Caemelbecke, E.; Guo, N.; Kadish, K. M. *Inorg. Chem.* **1996**, *35*, 6530.
(5) Witanowski, M.; Stefaniak, L.; Webb, G. A. *Nitrogen NMR Spectrosc., Annu. Rep. NMR Spectrosc.* **1993**, *25*, 1−480. Witanowski, M.; Stefaniak, L.; Webb, G. A. *Nitrogen NMR Spectrosc., Annu. Rep. NMR Spectrosc.* **1986**, *18*, 1−761. Witanowski, M.; Stefaniak, L.; Webb, G. A. *Nitrogen NMR Spectrosc., Annu. Rep. NMR Spectrosc.* **1981**, *11B*, 1−502. Witanowski, M.; Stefaniak, L.; Webb, G. A. *Nitrogen NMR Spectrosc., Annu. Rep. NMR Spectrosc.* **1977**, *7*, 117. Witanowski, M.; Stefaniak, L.; Webb, G. A. *Nitrogen NMR Spectrosc., Annu. Rep. NMR Spectrosc.* **1972**, *5*, 395. *Nitrogen NMR*; Witanowski, M., Webb, G. A., Eds.; Plenum: London, 1973.
(6) Annual reviews of nitrogen NMR: *Nuclear Magnetic Resonance: a Specialist Periodical Report*; Webb, G. A., Ed.; Royal Society of Chemistry: Cambridge, 1972−2001; Vols. 1−30 et seq. Shielding Tensors: Jameson, C. J.; et al. *Theoretical and Physical Aspects of Nuclear Shielding*; Royal Society of Chemistry: Cambridge.
(7) Mason, J. NMR spectroscopy of azo, azoxy and hydrazo compounds. In *The chemistry of the hydrazo, azo and azoxy groups*; Patai, S., Ed.; Wiley-Interscience: New York, 1997; Vol. 2, p 137.
(8) Richter-Addo, G. B.; Legzdins, P. Nitrogen NMR Spectroscopy. In *Metal Nitrosyls*; Oxford University Press: New York, 1992; p 58.
(9) Mingos, D. M. P.; Sherman, D. J. *Adv. Inorg. Chem.* **1989**, *34*, 293.
(10) Levy, G. C.; Lichter, R. L. *Nitrogen-15 Nuclear Magnetic Resonance Spectroscopy*; Wiley- Interscience: New York, 1979. Martin, G. J.; Martin, M. L.; Gouesnard, J.-P. *NMR Basic Princ. Prog.* **1981**, *18*.
(11) Randall, E. W.; Gillies, D. G. *Prog. NMR Spectrosc.* **1970**, *6*, 119. Roberts, J. D. *Bloch Festschrift*; Rice University Press: Houston, TX, 1980. Lichter, R. L. In *The Multinuclear Approach to NMR Spectroscopy*; Lambert, J. B., Riddell, F. G., Eds.; Reidel: Dordrecht, 1983; Chapter 10, p 207. von Philipsborn, W.; Müller, R. *Angew. Chem., Int. Ed. Engl.* **1986**, *25*, 383.
(12) Proctor, W. G.; Yu, F. C. *Phys. Rev.* **1950**, *77*, 717; **1951**, *81*, 20.
(13) Witanowski, M.; Stefaniak, L.; Webb, G. A. *J. Magn. Reson.* **1977**, *28*, 217. This paper compares reference standards. The publications of Witanowski, Webb, and co-workers use the nitromethane standard but give nitrogen *shieldings* (low-frequency positive) rather than *shifts* δ, so as to maintain consistency with their reports before the IUPAC sign convention of 1972 which changed the sign of the NMR shift.
(14) Kukolich, S. G. *J. Am. Chem. Soc.* **1975**, *97*, 5704.
(15) Jameson, A. K.; Jameson, C. J.; Opposunggu, D.; Wille, W.; Burrell P. M.; Mason, J. *J. Chem. Phys.* **1981**, *74*, 81.
(16) Ratcliffe, C. I.; Ripmeester, J. A.; Tse, J. S. *Chem. Phys. Lett.* **1983**, *99*, 177; Pestunovich, V. A.; Shterenberg, B. Z.; Lippmaa, E. T.; Myagi, M. Y.; Alla, M. A.; Tandura, S. N.; Boryshok, B. P.; Petukhov, L. P.; Voronkov, M. G. *Dokl. Akad. Nauk SSR* **1981**, *258*, 1410.
(17) Hunter, B. K. Brown, R. J. C. *J. Magn. Reson.* **1982**, *46*, 227.
(18) Kowalewski, J. *Annu. Rep. NMR Spectrosc.* **1990**, *22*, 307.
(19) Boeré, R. T.; Kidd, R. G. *Annu. Rep. NMR Spectrosc.* **1982**, *13*, 319.
(20) Bloembergen, N.; Purcell, E. M.; Pound, R. V. *Phys. Rev.* **1948**, *73*, 679.
(21) Gust, D.; Moon R. B.; Roberts J. D. *Proc. Natl. Acad. Sci.* **1975**, *72*, 4696. Dubin, S. B.; Clark N. A.; Bebedek, G. B. *J. Chem. Phys.* **1971**, *54*, 5158.
(22) Lapidot, A.; Irving, C. S. *J. Am. Chem. Soc.* **1977**, *99*, 5488.
(23) Levy, G. C.; Dechter, J. J.; Kowalewski, J. *J. Am. Chem. Soc.* 1978, **100**, 2308.
(24) Bammel, B. P.; Evilia, R. F. *Anal. Chem.* **1982**, *54*, 1318.
(25) Lippmaa, E.; Saluvere, T.; Laisaar, S. *Chem. Phys. Lett.* **1971**, *11*, 120.
(26) Giannini, D.; Armitage, I. M.; Pearson, H.; Grant D. M.; Roberts, J. D. *J. Am. Chem. Soc.* 1975, **97**, 3416.
(27) Lambert, J. B.; Netzel, D. A. *J. Magn. Reson.* **1977**, *25*, 531.
(28) Donovan-Mtunzi, S.; Hawkes, G. E.; MacDonald, C. J.; Mason, J.; Richards, R. L. J. *Chem. Soc., Dalton Trans.* **1985**, 2473.
(29) Loftus, P.; Bearden, W. H.; Roberts, J. D. *Nouv. J. Chim.* **1977**, *1*, 283.
(30) Schweitzer, D.; Spiess, H. W. *J. Magn. Reson.* **1974**, *16*, 243.
(31) Friedrich, J. O.; Wasylishen, R. E. *J. Chem. Phys.* **1985**, *83*, 3707.
(32) Hennig, J.; Limbach, H.-H. *J. Am. Chem. Soc.* **1984**, *106*, 292. Limbach, H.-H.; Hennig, J.; Kendrick R.; Yannoni, C. S. *J. Am. Chem. Soc.* **1984**, *106*, 4059. Limbach, H.-H.; Gerritzen, D.; Rumpel, H.; Wehrle, B.; Otting, G.; Zimmermann, H.; Kendrick R.; Yannoni, C. S. In *Photoreaktive Festkörper*; Karlsruhe, Germany, 1985.
(33) Noggle J. H.; Schirmer, R. E. *The Nuclear Overhauser Effect*; Academic Press: New York, 1971. Neuhaus D.; Williamson, M. *The Nuclear Overhauser Effect in Structural and Conformational Analysis*; VCH: Berlin, 1989.
(34) Hawkes, G. C.; Litchman W. M.; Randall, E. W. *J. Magn. Reson.* **1975**, *19*, 255.
(35) Freeman, R. *A Handbook of Nuclear Magnetic Resonance*; Longman: Harlow, 1987; p 157.
(36) Hiltunen, Y.; Jokisaari, J.; Lounila J.; Pulkkinen, A. *J. Am. Chem. Soc.* **1989**, *111*, 3217 and references therein.
(37) Bax, A.; Griffey R. H.; Hawkins, B. L. *J. Magn. Reson.* **1983**, *55*, 301.
(38) Schniksnis, R. A.; Opella, S. J. *J. Magn. Reson.* **1986**, *66*, 379.
(39) Roy, S.; Papastavaros, M. Z.; Sanchez V.; Redfield, A. G. *Biochemistry* **1984**, *23*, 4395.
(40) See, e.g., section 4.1 of the 1993 volume in ref 5.
(41) Kay, L. E.; Ikura, M.; Zhu. G.; Bax, A. *J. Magn. Reson.* **1991**, *91*, 422. Ikura, M.; Kay, L. E.; Krinks, M.; Bax, A. *Biochemistry*, **1991**, *30*, 5498.
(42) Freeman, R. *A Handbook of Nuclear Magnetic Resonance*; Longman: Harlow, 1987; p 14.
(43) Wasylishen R. E.; Friedrich, J. O. *J. Chem. Phys.* **1984**, *80*, 585.
(44) Lycka A.; Hansen, P. E. *Magn. Reson. Chem.* **1985**, *23*, 973.
(45) Risley J. M.; van Etten. L. *Methods Enzymol.* **1990**, *117*, 376.
(46) Mason, J.; Mingos, D. M. P.; Sherman, D.; Wardle, R. W. M. *J. Chem. Soc., Chem. Commun.* **1984**, 1223.
(47) Duthaler R. O.; Roberts, J. D. *J. Magn. Reson.* **1979**, *34*, 129.
(48) Alei, M.; Florin A. E.; Litchman, W. M.; *J. Am. Chem. Soc.* **1970**, *92*, 4828 and references therein.
(49) Mason J.; Christe, K. O. *Inorg. Chem.* **1983**, *22*, 1849.
(50) Haberkorn, R. A.; Stark, R. E.; van Willigen H.; Griffin, R. G. *J. Am. Chem. Soc.* **1981**, *103*. 2534.
(51) Ramanathan, K. V.; Opella, S. J. *Trans. Am. Cryst. Assoc.* **1988**, *24*, 145. Ramanathan, K. V.; Opella, S. J. *J. Magn. Reson.* **1990**, *86*, 227 and references therein.
(52) See, e.g.: Seo, Y.; Murakami, M. *Proc. R. Soc. London B* **1991**, *244*, 191.
(53) Smith, J. A. S. *Chem. Soc. Rev.* **1986**, *15*, 225**.**
(54) Shporer, M.; Ron G.; Navon, G. *Inorg. Chem.* **1965**, *4*, 358.
(55) Kintzinger, J.-P.; Lehn, J.-M. *Helv. Chim. Acta*, **1975**, *58*, 905.
(56) Martinengo, S.; Ciani, G.; Sironi, A.; Heaton, B. T.; Mason, J. *J. Am. Chem. Soc.* **1979**, *101*, 7095.
(57) Loewenstein, A. *J. Magn. Reson.* **1982**, *49*, 332.
(58) Gourdji M.; Guibé, L. *C. R. Acad. Sci. Paris* **1965**, *260*, 1131. Gourdji M.; Guibé, L.; Peneau, A. *J. Phys.* **1974**, *35*, 497. Nicholas, A. M. de P.; Wasylishen, R. E. *J. Phys. Chem.* **1985**, *89*, 5446.
(59) Loewenstein A.; Brenman, M. *J. Magn. Reson.* **1979**, *34*, 193.
(60) Moniz W. B.; Poranski, C. F. *J. Phys. Chem.* **1969**, *73*, 4145.
(61) Yamamoto Y.; Uzawa, J. *Chem. Lett.* **1978**, 1213.
(62) Moniz W. B.; Gutowsky, H. S. *J. Chem. Phys.* **1963**, *38*, 1155.
(63) Suchanski W.; Canepa, P. S. *J. Magn. Reson.* **1979**, *33*, 389.
(64) Pedersen, E. J.; Vold R. L.; Vold, R. R. *Mol. Phys.* **1980**, *41*, 811.
(65) Stark, R. E.; Vold, R. L.; Vold, R. R. *Chem. Phys.* **1977**, *20*, 337.
(66) Lippmaa, E.; Saluvere T.; Laisaar, S. *Chem. Phys. Lett.* **1971**, *11*, 120.
(67) Chew, K. F.; Derbyshire, W.; Logan, N.; Norbury, A. H.; Sinha, A. I. P. *J. Chem. Soc., Chem. Commun.* **1970**, 1708.
(68) Lehn, J.-M.; Kintzinger, J.-P. *Mol. Phys.* **1971**, *22*, 273.
(69) Loewenstein, A.; Waiman, R. *Mol. Phys.* **1973**, *25*, 49.
(70) Maliniak, A.; Kowalewski, J.; Panas, I. *J. Phys. Chem.* **1984**, *88*, 5628.
(71) Ancian B.; Tiffon, B. *J. Chem. Soc., Faraday Trans. 2* **1984**, *80*, 1067.

(72) Wasylishen, R. E.; Pettit, B. A. R.; Dong, Y. *J. Chem. Soc., Faraday Trans. 2* **1980**, *76*, 571.
(73) Szeverenyi, N. M.; Vold, R. R.; Vold, R. L. *Chem. Phys.* **1976**, *18*, 23, 31.
(74) Gillen K. T.; Noggle, J. H. *J. Chem. Phys.* **1970**, *52*, 4905.
(75) Tiffon B.; Ancian, B. *J. Chem. Phys.* **1982**, *76*, 1212.
(76) Lindman B.; Forsén, S. *NMR Basic. Princ. Prog.* **1976**, 12.
(77) Vold, R. R.; Vold R. L.; Szeverenyi, N. M. *J. Chem. Phys.* **1979**, *70*, 5213.
(78) Minelli, M.; Young C. G.; Enemark, J. H. *Inorg. Chem.* **1985**, *24*, 1111.
(79) Minelli, M.; Hubbard, J. L.; Christensen K. A.; Enemark, J. H. *Inorg. Chem.* **1983**, *22*, 2652.
(80) Chambers, O. R.; Harman, M. E.; Rycroft, D. S.; Sharp, D. W. A.; Winfield, J. M. *J. Chem. Res.* **1977**, (S) 150, (M) 1849.
(81) Bradley, D. C.; Hodge, S. R.; Runnacles, J. D.; Hughes, M.; Mason, J.; Richards, R. L. *J. Chem. Soc., Dalton Trans.* **1992**, 1663.
(82) Yamamoto, Y.; Uzawa, J. *Chem. Lett.* **1978**, 1213.
(83) Jordan, R. B. *J. Magn. Reson.* **1980**, *30*, 287. Hartmann H.; Sillescu, H. *Theor. Chim. Acta* **1964**, *2*, 371.
(84) Robert, J. M.; Evilia, R. F. *J. Am. Chem. Soc.* **1985**, *107*, 3733.
(85) Blanchard, A. A. *Inorg. Synth.* **1946**, *2*, 126.
(86) Groombridge, C. J.; Larkworthy, L. F.; Marécaux, A.; Mason, J.; Povey D. C.; Smith, G. W. *J. Chem. Soc., Dalton Trans.* **1992**, 3125.
(87) Brauer, G. *Handbook of Preparative Inorganic Chemistry*, 2nd ed.; Academic Press: New York, 1963; Vol. 1.
(88) Barnes, R. G.; Smith, W. V. *Phys. Rev.* **1954**, *93*, 95. Carlson, T. A.; Lu, C. C.; Tucker, T. S.; Nestor, W. W.; Malik, F. B. *Eigenvalues, radial expectation values, and potentials for free atoms from Z = 2 to 126*; Oak Ridge National Laboratory: Oak Ridge, 1970.
(89) Andersson, L.-O.; Mason, J.; van Bronswijk, J. W. *J. Chem. Soc. A* **1970**, 296.
(90) Evans, D. H.; Mason, J.; Mingos, D. M. P.; Richards, A. *J. Organomet. Chem.* **1983**, *249*, 293.
(91) Duffin, P. A.; Larkworthy, L. F.; Mason, J.; Stephens A. N.; Thompson, R. M. *Inorg. Chem* **1987**, *26*, 2034.
(92) Andersson, L.-O.; Mason, J.; van Bronswijk, J. W. *J. Chem. Soc., Chem. Commun.* **1968**, 99.
(93) Dilworth, J. R.; Kan, C.-T.; Richards R. L.; Stenhouse, I. A. *J. Organomet. Chem.* **1980**, *201*, C24.
(94) Bell, L. K.; Larkworthy, L. F.; Mason, J.; Mingos, D. M. P.; Povey, D. C.; Sandell B.; Tew, D. G. *J. Chem. Soc., Chem. Commun.* **1983**, 125.
(95) Scheidt, W. R.; Hoard, J. L. *J. Am. Chem. Soc.* **1973**, *95*, 8281. Cf. recent evidence of tilt/asymmetry in nitrosylmetalloporphyrin complexes: Ellison, M. K.; Scheidt, W. R. *J. Am. Chem. Soc.* **1997**, *119*, 7404. Ellison, M. K.; Scheidt., W. R. *Inorg. Chem.* **1998**, *37*, 382.
(96) Groombridge, C. J.; Larkworthy, L. F.; Mason, J. *Inorg. Chem.* **1993**, *32*, 379.
(97) Donovan-Mtunzi, S. Mason J.; Richards, R. L. *J. Chem. Soc., Dalton Trans.* **1984**, 1329.
(98) Donovan-Mtunzi, S.; Mason, J.; Richards, R. L. *J. Chem. Soc., Dalton Trans.* **1984**, 469.
(99) (a) Mingos, D. M. P. *Inorg. Chem.* **1973**, *12*, 1209. (b) Hoffman, R.; Chen, M. M. L.; Elian, M.; Rossi, A, R.; Mingos, D. M. P. *Inorg. Chem.* **1974**, *13*, 2666. (c) Eisenberg, R.; Meyer, C. *Acc. Chem. Res.* **1975**, *8*, 26.
(100) Mason, J. Nitrogen Shielding Tensors. In *Nuclear Magnetic Shielding and Molecular Structure*; Tossell, J. A., Ed.; NATO ASI Series C: Mathematical and Physical Sciences; Kluwer: Dordrecht, 1993; Vol. 386, p 449.
(101) Mason, J.; Mingos, D. M. P.; Schaefer, J.; Sherman, D.; Stejskal, E. O. *J. Chem. Soc., Chem. Commun.* **1985**, 444.
(102) Casleton, K. H.; Kukolich, S. G. *J. Chem. Phys.* **1975**, ***62***, 2696. Bhattacharyya, P. K.; Dailey, B. P. *J. Chem. Phys.* **1973**, *59*, 5820.
(103) Western, C. M.; Langridge-Smith, P. R. R.; Howard, B. J.; Novick, S. E. *Mol. Phys.* **1981**, *44*, 145.
(104) Kukolich, S. G. *J. Am. Chem. Soc.* **1982**, *104*, 69279.
(105) Schweitzer, D.; Spiess, H. W. *J. Magn. Reson.* **1974**, *16*, 243. Stark, R. E.; Vold, R. L.; Vold, R. R. *Chem. Phys.* **1977**, *20*, 337.
(106) Gibby, M. G.; Griffin, R. G.; Pines, A.; Waugh, J. S. *Chem. Phys. Lett.* **1972**, *17*, 80.
(107) Garvey, R. M.; F. C. De Lucia, F. C. *J. Mol. Spectrosc.* **1974**, *50*, 38.
(108) Chan, S. I.; Baker, M. R.; Ramsey, N. F. *Phys. Rev. A* **1964**, *136*, 1224. Baker, M. R.; Anderson, C. H.; Ramsey, N. F *Phys. Rev. A* **1964**, *133*, 1533. Ishol L. M.; Scott, T. A. *J. Magn. Reson.* **1977**, *27*, 23.
(109) Malli, G.; Froese, C. *Int. J. Quantum Chem. Suppl.* **1967**, *1*, 95.
(110) Laska, T. E.; Root, T. W. **1989**, quoted by *A Compilation of Chemical Shift Anisotropies*; Duncan, T. M., Ed.; Farragut Press: Chicago, 1990; p N-4. Solution spectrum: Stevens, R. E.; Gladfelter, W. L. *Inorg. Chem.* **1983**, *22*, 2034.
(111) Barrie, P. J.; Groombridge, C. J.; Larkworthy L. F.; Mason, J. Unpublished work.
(112) Mahnke, H.; Sheline, R. K.; Spiess, H. W. *J. Chem. Phys.* **1974**, *61*, 55−60.
(113) Gleeson J. W.; Vaughan, R. W. *J. Chem. Phys.* **1983**, *78*, 5384.
(114) Buchner W.; Schenk, W. A. *Inorg. Chem.* **1984** *23*, 132.
(115) Brown, D. A.; Chester, J. P.; Fitzpatrick, N. J.; King, I. J. *Inorg. Chem.* **1977**, 16, 2497. Brown, D. A.; Chester, J. P.; Fitzpatrick, N. J. *Inorg. Chem.* **1982**, *21*, 2111
(116) Braterman, P. S.; Milne, D. W.; Randall, E. W.; Rosenberg, E. *J. Chem. Soc., Dalton Trans.* **1973**, 1027.
(117) Lumsden, M. D.; Wu, G.; Wasylishen, R. E.; Curtis, R. D. *J. Am. Chem. Soc.* **1993**, *115*, 2825.
(118) Scheidt, W. R.; Hoard, J. L. *J. Am. Chem. Soc.* **1973**, *95*, 8281. Cf. recent evidence of tilt/asymmetry in nitrosylmetalloporphyrin complexes: Ellison, M. K.; Scheidt, W. R. *J. Am. Chem. Soc.* **1997**, *119*, 7404. Ellison, M. K.; Scheidt., W. R. *Inorg. Chem.* **1998**, *37*, 382.
(119) Kukolich, S. G. *J. Am. Chem. Soc.* **1982**, *104*, 6927.
(120) Mason, J. Unpublished work.
(121) Andersson, L.-O.; Mason, J. *Chem. Commun.* **1968**, 99.
(122) Western, C. M.; Langridge-Smith, P. R. R.; Howard, B. J.; Novick, S. E. *Mol. Phys.* **1981**, *44*, 145.
(123) Ditchfield, R. *Mol. Phys.* **1974**, *27*, 789.
(124) Kutzelnigg; W.; Fleischer, U.; Schindler, M. In *NMR Basic Principles and Progress*; Springer: Berlin, Heidelberg, 1990; Vol. 23, p 165.
(125) Hansen, Aa. E.; Bouman, T. D. *J. Chem. Phys.* **1985**, *82*, 5035.
(126) Keith, T. A.; Bader, R. F. W. *Chem. Phys. Lett.* **1993**, *210*, 223.
(127) Schindler, M.: Kutzelnigg, W. *Mol. Phys.* **1992**, *48*, 781
(128) Cheeseman, J. R.; Trucks, G. W.; Keith, T. A.; Frisch, M. J. *J. Chem. Phys.* **1996**, *104*, 5497.
(129) van Wüllen, C.; Kutzelnigg, W. *J. Chem. Phys.* **1996**, *104*, 2330.
(130) Moore, E. A. *Chem. Phys. Lett.* **2000**, *317*, 360.
(131) Barrie, P. J.; Groombridge, C. J.; Mason, J.; Moore, E. A. *Chem. Phys. Lett.* **1994**, *219*, 491.
(132) Lumsden, M. D.; Wu, G.; Wasylishen, R. E.; Curtis, R. D. *J. Am. Chem. Soc.* **1993**, *115*, 2825.
(133) de Dios, A. C.; Roach, J. L. *J. Phys. Chem. A* **1999**, *103*, 3062.
(134) Godbout, N.; Sanders, L. K.; Salzmann, R.; Havlin, R. H.; Wojdelski, M.; Oldfield, E. *J. Am. Chem. Soc.* **1999**, *121*, 3829. Cf. Salzmann, R.; Wojdelski, M.; McMahon, M.; Havlin, R. H.; Oldfield, E. *J. Am. Chem. Soc.* **1997**, *120*, 1349.
(135) Mason, J.; Moore, E. A. *J. Mol. Struct.* **2002**, *602−3*, 347−356.
(136) Kowalewski, J. *Annu. Rep. NMR. Spectrosc.* **1982**, *12*, 82. Kowalewski, J. *Prog. NMR Spectrosc.* **1977**, *11*, 1. Freyer, W. *Z. Chem.* **1981**, *21*, 47. Mason, J. Nitrogen. In *Multinuclear NMR*; Mason, J., Ed.; Plenum: New York, 1987: Chapter 12, p 357. Mason, J. *Encyclopedia of Nuclear Magnetic Resonance*; Wiley: New York, 1996; Vol. 5, pp 3241−3244
(137) Robert, J. M.; Evilia, R. F. *J. Am. Chem. Soc.* **1985**, *107*, 3733.
(138) Schulman, J. M.; Venanzi, T. J. *J. Am. Chem. Soc.* **1976**, *98*, 4701.
(139) Schulman, J. M.; Venanzi, T. J. *J. Am. Chem. Soc.* **1976**, *98*, 6739. Lee, W. S.; Schulman, J. M. *J. Am. Chem. Soc.* **1979**, *101*, 3182.
(140) (a) Schulman, J. M.; Ruggio, J.; Venanzi, T. *J. Am. Chem. Soc.* **1977**, *99*, 2045; ref 139.
(141) Hilton, J.; Sutcliffe, L. H. *Prog. NMR Spectrosc.* **1975**, *10*, 2. Gil, V. M. S.; von Philipsborn, W. *Magn. Reson. Chem.* **1989**, *27*, 409. Contreras, R. H.; Natiello M. A.; Scuseria, G. E. *Magn. Reson. Rev.* **1985**, *9*, 239.
(142) Schultheiss, H.; Flück, E. *Z. Naturforsch.* **1977**, *32B*, 257.
(143) Bundgaard, T.; Jakobsen H. J.; Rahkamaa, E. J. *J. Magn. Reson.* **1975**, *19*, 345.
(144) (a) Schulman, J. M.; Venanzi, T. J. *J. Am. Chem. Soc.* **1976**, *98*, 6739. Lee, W. S.; Schulman, J. M. *J. Am. Chem. Soc.* **1979**, *101*, 3182. (b) Schurko, R. W.; Wasylishen, R. E. *J. Phys. Chem. A* **2000**, *104*, 3410.
(145) Martin, M. L.; Sun X. Y.; Martin, G. J. *Annu. Rep. NMR Spectrosc.* **1985**, *16*, 188.
(146) Ridd, J. H.; Trevellick S.; Sandall, J. P. B. *J. Chem. Soc., Perkin Trans. 2*, **1992**, 1535.
(147) Bubnov, N. N.; Bilevitch, K. A.; Poljakova L. A.; Okhlobystin, O. Yu. *J. Chem. Soc., Chem. Commun.* **1972**, 1058.
(148) Dreher, E. L.; Niederer, P.; Rieker, A.; Schwarz W.; Zollinger, H. *Helv. Chim. Acta.* **1981**, *64*, 488.
(149) Grigor'ev, I. A.; Volodarsky, L. B.; Gogolev A. Z.; Sagdeev, R. Z. *Chem. Phys. Lett.* **1985**, *122*, 46.

CR000075L